



**ANLECR&D project**

**Milestone Report for Project 6-0710-0061 on “Gas quality impacts,  
assessment and control in oxy-fuel technology for CCS”**

**The feasibility of impurity control during  
compression of oxy-fuel flue gas: removing  
NO<sub>x</sub> and SO<sub>x</sub> as acid condensates**

by

Rohan Stanger, Timothy Ting and Terry Wall

Chemical Engineering, the University of Newcastle, NSW, Australia

August 2012

## ***Acknowledgments***

The authors wish to acknowledge financial assistance provided through Australian National Low Emissions Coal Research and Development (ANLEC R&D). ANLEC R&D is supported by Australian Coal Association Low Emissions Technology Limited and the Australian Government through the Clean Energy Initiative.

## **Table of Contents**

Acknowledgments.....	2
List of Figures .....	4
List of Tables .....	5
EXECUTIVE SUMMARY .....	6
1. Introduction.....	13
1.1 Carbon capture and storage.....	14
1.2 CO <sub>2</sub> Capture technologies .....	14
1.3 Oxy-fuel development .....	16
1.4 Callide Oxyfuel Project.....	17
1.4 Flue gas impurities in oxy-fuel combustion.....	19
1.6 Oxy-fuel impurities during compression .....	21
1.7 NO oxidation mechanisms .....	22
2. Project objectives .....	25
3. Experimental .....	26
3.1 Apparatus .....	26
3.2 Experiments .....	27
4. Results.....	28
4.1 Dry NO <sub>x</sub> System .....	28
4.2 Wet NO <sub>x</sub> System .....	30
4.3 Wet SO <sub>x</sub> /NO <sub>x</sub> system.....	31
4.4 Thermodynamics.....	33
4.6 Final comments .....	35
5. Future Work.....	37
6. Conclusion .....	38
Appendix.....	41
References.....	43

## **List of Figures**

Figure 1. IEA projections for world CO <sub>2</sub> emissions and key abatement options.....	13
Figure 2. Federal Treasury modelling for projected Australian CO <sub>2</sub> emissions and their sources .....	14
Figure 3. Main technologies for CO <sub>2</sub> capture from coal fired electricity generators.....	16
Figure 4. Historical development of Oxy-fuel combustion .....	17
Figure 5. Diagram of the Callide Oxyfuel Project .....	19
Figure 6. Diagram of Vattenfall’s Schwarze Pumpe Oxyfuel pilot plant.....	19
Figure 8. Callide Oxy-fuel compression circuit, from [15] .....	21
Figure 8. Interaction of NO <sub>x</sub> , SO <sub>x</sub> and Hg during compression of oxy-fuel flue gas .....	22
Figure 9. NO <sub>x</sub> oxidation and absorption mechanisms. ....	23
Figure 10. Comparison of solubilities of NO <sub>x</sub> and SO <sub>x</sub> gaseous species in water using Henry’s Constant.....	23
Figure 11. Pressurised laboratory apparatus for contacting NO <sub>x</sub> gases with water.....	27
Figure 12. Effect of pressure on the oxidation of NO to NO <sub>2</sub> (in 4% O <sub>2</sub> ) without water.....	29
Figure 13. Comparison of NO <sub>x</sub> conversion in reactor and transport lines showing effect of residence time .....	29
Figure 14. Evaluation of global kinetic model to measured experimental results.....	30
Figure 15. Gaseous NO <sub>x</sub> concentrations after contacting water at different pressures. Lines in grey compare the dry experimental results .....	31
Figure 16. Aqueous NO <sub>x</sub> species present in the water after continuous contact with the gas stream for either 10 minutes or 8 hr “pseudo-equilibrium” conditions.....	31
Figure 17. Aqueous NO <sub>x</sub> and SO <sub>x</sub> species present in solution. ....	32
Figure 18. Thermodynamic modelling of dry NO <sub>x</sub> system.....	34
Figure 19. Thermodynamic modelling of gas species in wet NO <sub>x</sub> system .....	35

Figure 20. Thermodynamic modelling of aqueous species in wet NO<sub>x</sub> system .....35

**List of Tables**

TABLE 1. Reactions and Equilibrium values for Counce and Perona NO<sub>x</sub> mechanisms [25] .....41

TABLE 2. Solubility values for NO<sub>x</sub> and SO<sub>x</sub> species [26] at 25°C.....42

## ***EXECUTIVE SUMMARY***

Amongst the three carbon capture and storage (CCS) technologies (Integrated gasification combined cycle or pre-combustion - IGCC-CCS; post combustion capture or post-combustion - PCC and oxy-fuel) being progressed through demonstrations, the CO<sub>2</sub> gas quality has the greatest potential variability, uncertainty and impact in oxy-fuel. The cost of the gas quality control operations and process energy requirements may potentially be minimized and CO<sub>2</sub> recovery optimized, but at present the technical possibilities are still being established by studies such as the present research.

The CO<sub>2</sub> impurities from oxy-fuel technology for CCS differ greatly from pre- and post-combustion technologies for CCS in quality and quantity, having higher levels of gas impurities which impact efficiency and operation such as sulfur oxides (SO<sub>2</sub>, SO<sub>3</sub>), nitrogen oxides, (NO, NO<sub>2</sub>), and mercury gases (as atomic or oxidised, Hg<sup>0</sup> and Hg<sup>++</sup>).

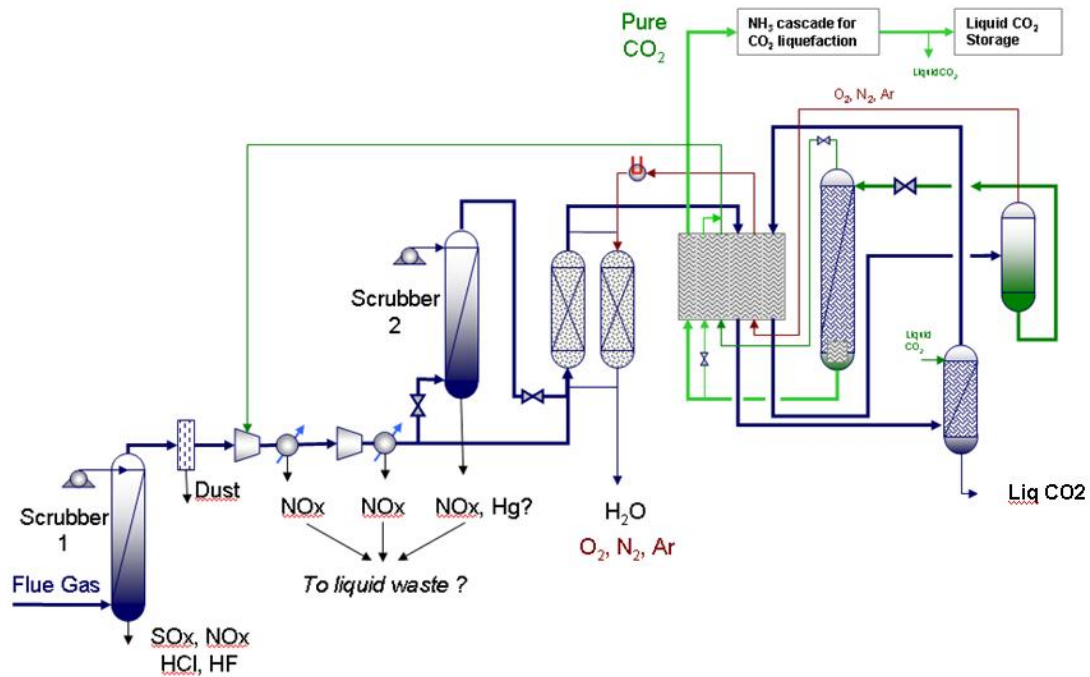
Options are available for gas quality control in the furnace, by conventional flue gas cleaning and in the CO<sub>2</sub> processing unit (CPU).

Australian power plants do not have cleaning units for sulfur, nitrogen or mercury gas species. Therefore, the application of oxy-fuel technology in Australia requires a greater understanding of costs and impacts associated with the expected higher impurity levels fed to the CPU. For example, in a oxy-fuel retrofit, the possible need for a sulfur gas removal unit (using standard flue gas desulphurization (FGD) technology based on calcium solutions) prior to the CPU for high sulfur coals, is associated with a plant capital cost increase of about 7.5%. For Australian oxyfuel plants, the concentration of SO<sub>2</sub> in flue gas will also be higher, typically 500-1500ppm compared to concentrations less than 100ppm where an FGD is included.

The removal of SO<sub>x</sub> and NO<sub>x</sub> species prior to CO<sub>2</sub> liquefaction is necessary to reduce the effects of corrosion during CO<sub>2</sub> transport and lower the health risk in the event of a

gas leak. The removal of mercury species prior to CO<sub>2</sub> liquefaction is critical in preventing corrosion in the cryogenic heat exchanger.

Scrubbing units have been included in the major CPU flowsheets by Air Liquide, Linde, Praxair and Air Products. The basic design of the CPU which was developed by Air Liquide for the Callide Oxy-fuel Project (COP) is given in the schematic below. The schematic shows that the flue gas (following the recycled gas line after the existing bag filter unit at Callide) is first fed into a quench/scrubber column operating at atmospheric pressure (noted as scrubber 1) primarily to condense water and remove SO<sub>2</sub>, as well as other soluble acid gases, with aqueous NaOH used as a chemical agent for SO<sub>2</sub> recovery.



After dust cleaning, the schematic shows that flue gas is compressed (to a pressure of about 20 bar). During compression, nitric oxide (NO) reacts with oxygen to form NO<sub>2</sub>, which is absorbed by condensed moisture to form HNO<sub>2</sub> or HNO<sub>3</sub>. The resulting liquid waste is transported to the ash pit. Mercury is expected to be oxidized and dissolved in the high pressure condensate. Overall, it is expected that NO<sub>2</sub> is removed as an acid and residual mercury is removed as a nitrate which is Hg(NO<sub>3</sub>)<sub>2</sub>.

This report provides an assessment of  $\text{NO}_x$  and  $\text{NO}_x/\text{SO}_x$  mixture behaviour under pressure in controlled wet and dry conditions and is part of a larger study on the interaction of  $\text{NO}_x$  with  $\text{SO}_x$  as well as Hg in a wet environment, such as during compression. The apparatus used similar to that used in previous work performed in a study by Air Products and Imperial College [1, 2].

### **Project objectives**

*The objective is to establish the feasibility of  $\text{CO}_2$  gas quality control in oxy-fuel technology by removal of sulfur oxide and nitrogen oxide gas impurities during compression in condensates from the flue gas moisture as liquid acids .*

The objective would be achieved by building an experimental rig for testing of  $\text{CO}_2$  compression, and undertaking laboratory experiments on the impurity removal.

The focussing questions for the experiments undertaken have been based on the mechanisms by which the impurities are expected to be removed, namely:

- *What is the extent of oxidation of the primary nitrogen oxide -  $\text{NO}$  - in flue gas to soluble  $\text{NO}_2$  during compression?*
- *What is the possibility of interference of the nitrogen chemistry to form  $\text{NO}_2$  by  $\text{SO}_2$ ?*
- *Are sulphur gases absorbed to form a liquid acid –  $\text{H}_2\text{SO}_4$  - in addition to  $\text{HNO}_3$ ?*
- *Is  $\text{SO}_x$  absorption catalysed by the formation of higher nitrogen oxides, in particular  $\text{NO}_2$ , and does it occur in the gas or aqueous phase?*

### **Compression conditions**

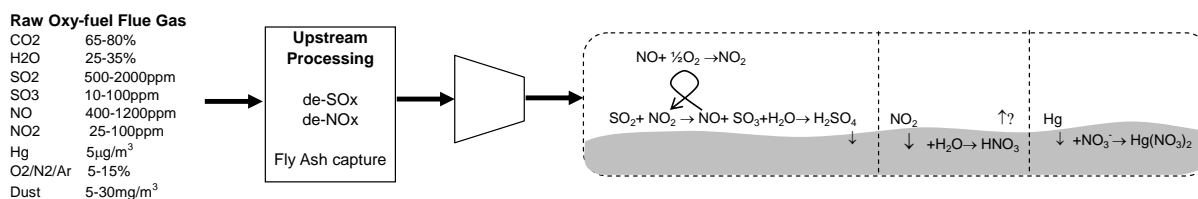
The oxy-fuel flue gas entering the compression train is expected to be partially cleaned of acid gases, having passed through the atmospheric caustic scrubber. At the COP, compression occurs in a four stage compressor with two intercoolers to remove

condensates. Following compression the gas is then contacted with chilled water in a high pressure packed column to further remove  $\text{NO}_x$  species. This means that there is potentially two condensate streams produced in the coolers after stages 2 and 3 (at a pressure of 6 bar) and after the 4<sup>th</sup> stage (at 25 bar). Modelling this process is complicated by the unknown level of gas-liquid contact during the compression stages and the challenge of introducing continuous gas and liquid streams under pressure. From the pilot IHI results on oxy-fuel combustion,  $\text{NO}_x$  levels in the raw flue gas varied between 550-900ppm, though this concentration will vary with coal and operating conditions. It is expected that the main  $\text{NO}_x$  species entering the compression train is NO as  $\text{NO}_2$  is most likely removed during caustic scrubbing.

### **Literature and theory on gas scrubbing for $\text{SO}_x$ , $\text{NO}_x$ and Hg**

Previous oxy-fuel pilot studies have suggested that compression of raw flue gas has the potential to remove  $\text{NO}_x$  and  $\text{SO}_x$  from the gas by the formation of acidic condensates. This is thought to occur principally via the “lead chamber process” involving high pressure NO oxidation followed by catalytic  $\text{SO}_2$  oxidation by  $\text{NO}_2$ . The oxidation of NO has been used for the production of nitric acid to pressures of up to 10 bar and previous modelling of oxy-fuel compression has suggested that the equilibrium with nitrates in the liquid will control the overall  $\text{NO}_x$  conversion. Previous work has not indicated the extent to which  $\text{SO}_x$  delays the NO conversion. Experience with mercury comes from the natural gas industry where trace amounts are scrubbed with activated carbon prior to cryogenic processing. Flue gases from coal-firing plants are different in their composition, especially that it contains both oxygen and water vapour. The extent to which mercury is removed in nitric acid is uncertain, though mercuric nitrate,  $\text{Hg}(\text{NO}_3)_2$ , is often used as a standard solution in analytical laboratories in place of elemental Hg, which is insoluble.

Related to the focussing questions, the literature indicates that the simplified mechanism in the following schematic will result in the conversion of NO and  $\text{SO}_2$  to sulphuric and nitric acids during  $\text{CO}_2$  compression involving condensation of water.



The mechanism involves the following four steps, the first three related to the focussing questions of the current study: NO reacts with O<sub>2</sub> to NO<sub>2</sub> at high pressure; NO<sub>2</sub> reacts with SO<sub>2</sub> to form SO<sub>3</sub> then H<sub>2</sub>O to liquid H<sub>2</sub>SO<sub>4</sub>; residual NO<sub>2</sub> reacts with H<sub>2</sub>O to form liquid HNO<sub>3</sub>; mercury can then react with HNO<sub>3</sub> to Hg(NO<sub>3</sub>)<sub>2</sub>

### Experimental methodology

An experiment was devised to provide measurements of NO conversion to NO<sub>2</sub> and acid formation at pressures up to 30 bar, with an assessment of interference by SO<sub>x</sub>. A wet system was used which continuously bubbled a stream of NO<sub>x</sub> gases through a set volume of water in a short bubble column. Gases were passed through the liquid for 10 minutes with continuous analysis of the off-gas. Batch liquid analyses were determined on the final liquid. Several experiments were also conducted with an 8 hour contact time as a comparison.

### Experimental and mechanistic findings

Current single step kinetic NO<sub>x</sub> conversion models were found to adequately describe the oxidation of NO to NO<sub>2</sub> in a dry process. The wet pressurised conditions significantly reduced the amount of NO<sub>2</sub> exiting the reactor, producing nitrate and nitrite species in the liquid phase. In common with other results in the literature, it was found that the amount of NO<sub>x</sub> removed from the gas stream could not be accounted for by the nitrogen species from the liquid analysis. Results from the mixed SO<sub>x</sub>/NO<sub>x</sub> wet system indicated that the use of 1000ppm SO<sub>2</sub> resulted in interference with the NO<sub>2</sub> gas measurement. Liquid analysis of the mixed system indicated that SO<sub>x</sub> were absorbed in either atmospheric conditions or at 20bar. Intermediate pressures (5, 10, 15 bar) produced similar NO<sub>x</sub> absorption to conditions without SO<sub>2</sub>.

## **Conclusions and practical implications for compression of oxy-fuel flue gas**

The experiments have established the feasibility of CO<sub>2</sub> gas quality control in oxy-fuel technology by removal of sulfur oxide and nitrogen oxide gas impurities during compression in condensates as liquid acids.

From dry experiments, it is concluded the extent of oxidation of insoluble NO to soluble NO<sub>x</sub> was found to exceed 90% above a pressure of 15 bar. This oxidation was found to be kinetically limited and could be predicted using a single global reaction scheme. The extent to which NO is oxidized in an oxy-fuel compression train will therefore depend on the residence time and pressure within each compression stage.

From wet experiments involving contact with liquid water and water vapour, it is concluded that at the saturated conditions and pressures in an oxyfuel compression circuit, a significant conversion of NO to higher order oxides can be expected. Such oxides are more soluble than either NO or NO<sub>2</sub> and thus would most likely react with the condensate to form liquid acids.

From wet experiments involving NO<sub>x</sub>/SO<sub>x</sub>, it is concluded that during multi-stage CO<sub>2</sub> compression it is likely that SO<sub>2</sub> will be removed during early stages along with most of the water vapour. At pressures below 20 bar, NO oxidation and absorption to form acid may be restricted by the existence of SO<sub>x</sub>.

The experiments have revealed that the mechanism suggested by the literature is indeed simplified, in that additional nitrogen and sulphur species exist as gases and liquids. The extent to which these additional nitrogen and sulphur species form (or are) acids or other liquid products may be inferred, but further work is needed to clarify their chemistry.

## **Future Work**

In future laboratory experiments, it is clear that future research should focus on the closure of the nitrogen mass balance in the wet system with particular attention

focussed on identification of missing species. The addition of water to the system has currently been through bubbling conditions, however future experiments could also include water as a vapour only for comparison to indentify gas phase mechanisms. Ultimately, the mixed gas system should also include an assessment of gas phase mercury absorption into a liquid containing HNO<sub>3</sub>. Addition of oxygen and substituting carbon dioxide for the nitrogen used to date is also recommended.

## 1. Introduction

The increase of CO<sub>2</sub> in the atmosphere is considered to be associated with global warming [3]. Anthropogenic sources of CO<sub>2</sub>, in particular the combustion of fossil fuels, makes up the dominant proportion of global emissions [3]. However, energy supply underpins stable economic growth and given the expected rise in population and energy demand over the next 25 years, the continued reliance on fossil fuels is expected [4]. A recent MIT study concluded that carbon capture and storage is a critical enabling technology allowing coal to meet future energy demands [5] while reducing overall CO<sub>2</sub> emissions. It is also considered a key technology in the IEA's roadmap for decarbonising the world's energy sector [6] (shown in Figure 1). In Australia, coal is a major export commodity and contributes almost 80% of domestic electricity. As such, efforts to reduce CO<sub>2</sub> emissions without carbon capture and storage will have a significant impact on Australian industries and national economy (eg replacement of current coal fired generating capacity, widespread reduction in mining sector). Figure 2 shows the Australian treasury modelling of CO<sub>2</sub> emissions with/without a carbon price [7]. Under a carbon price, the generation of electricity can be observed to produce the largest contribution to CO<sub>2</sub> mitigation, outside of (as yet) undefined offshore abatement options. Further modelling of technology adoption in Australia suggests that by 2050 there will be no coal fired electricity production without CCS.

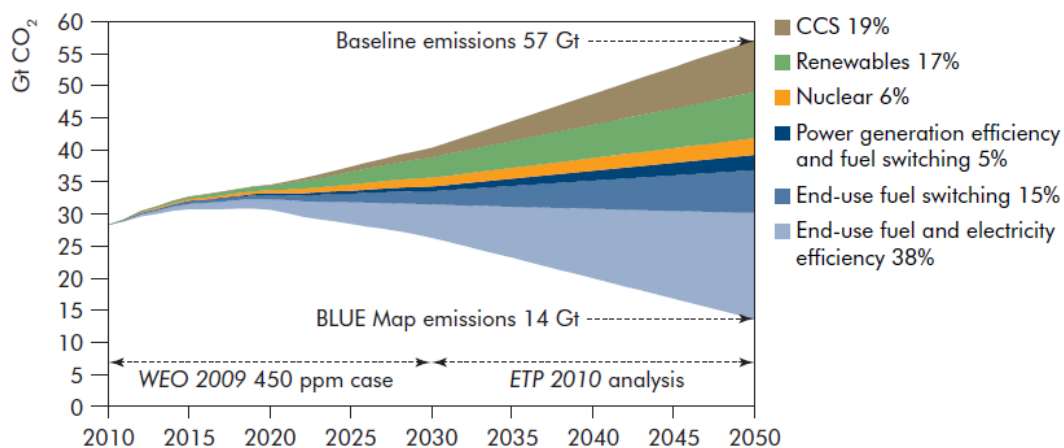


**Figure 1.** IEA projections for world CO<sub>2</sub> emissions and key abatement options

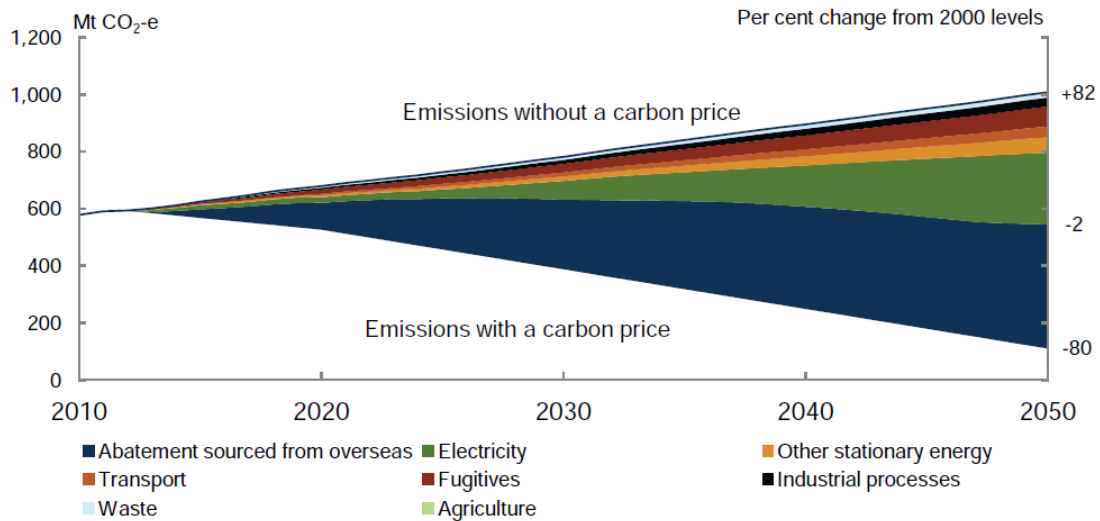


**Figure 2.** Federal Treasury modelling for projected Australian CO<sub>2</sub> emissions and their sources

### 1.1 Carbon capture and storage

The concept of CO<sub>2</sub> capture and storage is not new. It was originally suggested as a means of enhancing oil recovery (EOR) in depleted oil wells. By re-injecting the CO<sub>2</sub> (naturally present in crude oil) back into the top of the well, the pumping requirements to get the oil to the surface were reduced through reduced head pressure and lower oil viscosity. The concept, involves capturing CO<sub>2</sub> from fossil fuel combustion and pumping it underground. Under this scenario, the CO<sub>2</sub> is injected as a supercritical fluid (allowing pumping like a liquid but compression like a gas) into a geologically stable formation, typically at depths below 1000m. In Australia, large scale testing of CO<sub>2</sub> injection is currently underway on the Victorian Otway basin [8] and has found no major hurdles to both geological considerations and public stakeholder acceptance.

### 1.2 CO<sub>2</sub> Capture technologies

The abatement of CO<sub>2</sub> from stationary power generators has three main technology options to capture the gas in a form suitable for storage underground [9]; Post-combustion capture (PCC), Integrated Gasification & Combined Cycle with CCS (IGCC-CCS), and Oxy-fuel combustion. These three capture processes are shown in Figure 3 with the red boxes indicating additional equipment required. The relative merits of each technology option and possible detractors are reviewed by Wall [9]. As a summary, both PCC and Oxyfuel can be retrofitted to existing utilities, while only IGCC-CCS has the potential to produce H<sub>2</sub> for synthetic fuel production. Importantly,

each technology has yet to be commercially applied at large scale. Oxy-fuel combustion occurs in a mixture of oxygen and recycled CO<sub>2</sub>, such that the dominant product after combustion is CO<sub>2</sub>. The higher concentration of CO<sub>2</sub> in the flue gas allows direct liquefaction of the flue gas to produce a liquid CO<sub>2</sub> product. The flue gas is recycled because combustion in pure oxygen produces excessive flame temperatures and does not sufficiently carry the heat through the convective pass in the boiler (where the steam is superheated). In retro-fit circumstances, the extent of recycle is determined by heat transfer considerations, in that this must be matched to that at air-firing. The main benefits of this process are that it operates in a similar manner to typical air fired operations, does not alter the existing steam cycle (as does PCC for solvent regeneration) and uses industrially mature technologies in the form of air separation and compression equipment. An issue with oxy-fuel is that it produces higher concentrations of flue gas impurities in the boiler, and these gases must be substantially removed before CO<sub>2</sub> transport and storage.

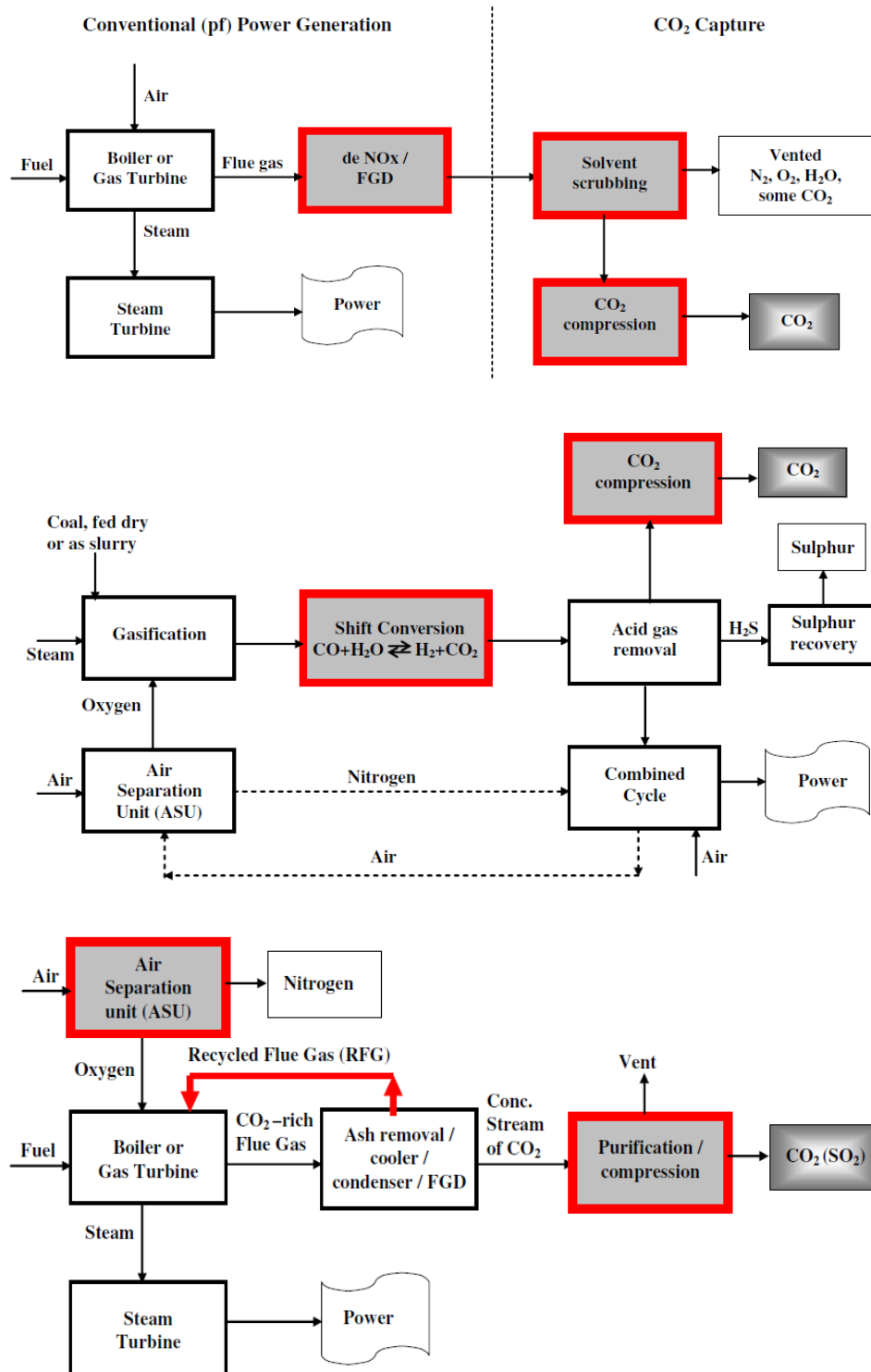


**Figure 3.** Main technologies for CO<sub>2</sub> capture from coal fired electricity generators; post combustion capture (top), Integrated Gasification & Combined Cycle-CCS (middle) and oxy-fuel combustion (bottom).

### 1.3 Oxy-fuel development

While the public support for CO<sub>2</sub> abatement is somewhat uncertain, the industrial sector has been driving the development of oxy-fuel towards demonstration. Figure 4 shows the historical development of oxy-fuel technology. The vertical scale represents the

scale of electrical output, traditionally taken as 30% of the theoretical thermal size. However almost all projects shown are relatively small in size and would not include electrical generation. Oxy-fuel testing facilities are operated by a number of boiler manufacturers (Alstom, Babcock and Wilcox, Doosan). However, the construction of a full chain pilot plant in Schwarze Pumpe by Vattenfall in 2008 marked a major milestone for the technology and its subsequent operation has allowed the testing of a number of burner designs and given real experience in capturing CO<sub>2</sub> as a liquid product. The next major milestone for the technology has been the Callide Oxyfuel project which went into operation in 2012. As can be observed in Figure 4, the Callide Oxyfuel Project represents a critical step forward from pilot scale (eg Schwarze Pumpe) to large demonstration scale (eg FutureGen 2.0 and Compostilla) The project will demonstrate the first semi-commercial electrical generation using oxy-fuel and will give experience in continuous operation under real electrical demand. Industrial (larger scale) demonstrations are planned for 2015 in the US based FutureGen 2.0 and in Europe with the Spanish Compostilla CFB300 project.

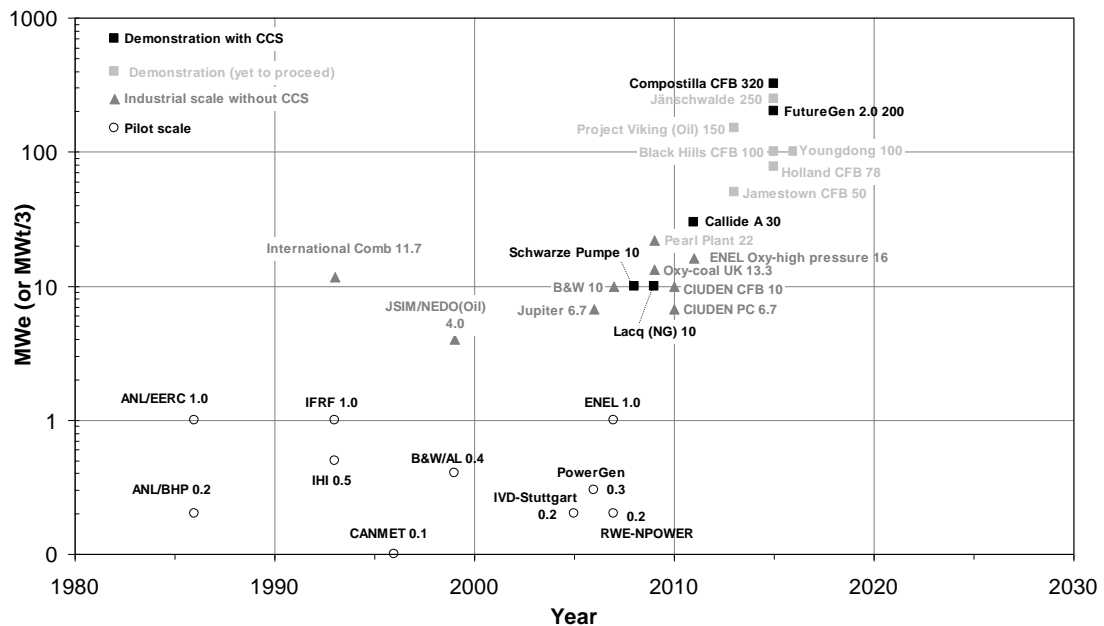


**Figure 4.** Historical development of Oxy-fuel combustion

#### 1.4 Callide Oxyfuel Project

The Callide Oxy-fuel Project is based in Biloela, Queensland Australia. It began in 2003 as a Australian/Japanese collaboration involving CS Energy, IHI and the University of Newcastle. The feasibility study was undertaken from 2004 to 2007. The

project involves retrofitting a 30MW sub-critical boiler with flue gas recycle + heat exchangers, a Air Separation Unit (ASU) and a CO<sub>2</sub> purification plant (Figure 5). The liquefied CO<sub>2</sub> will potentially be transported by truck to a sequestration site. The existing air fired circuit is relatively unique compared to other power stations elsewhere in the world in that the flue gas is does not pass through de-NO<sub>x</sub> and de-SO<sub>x</sub> removal units. Instead, the plant relied on using low sulfur (and mercury) coals and lenient Australian environmental regulations. This type of circuit is common in Australia due to the quality of coal used in domestic power generation and the sparsely populated areas in which they are located. This process is an example of a “low sulfur” (ie Fuel-S<1%) oxy-fuel flow sheet and represents the lowest cost approach for a retrofit application.

In Europe, USA and Japan, the more common flue gas circuit involves secondary NO<sub>x</sub> removal (such as ammonia injection or the use of solid catalysts) and flue gas desulfurisation units (FGD). Thus there are variations in process equipment and therefore gas compositions.

The Vattenfall Schwarze Pumpe oxy-fuel pilot plant, shown in Figure 6, is an example of an oxy-fuel flow sheet involving these extra cleaning stages. Such additional environmental units are expensive and add to the overall costs of plant and electricity production. Consequently, Australia has the potential to deploy cheaper electricity using oxy-fuel technology if these flue gas impurities can be managed in the CO<sub>2</sub> compression system. Conversely, a failure to handle flue gas species (such as SO<sub>x</sub>, NO<sub>x</sub> and Hg) could require additional environmental units to be added thereby increasing the cost of deployment.

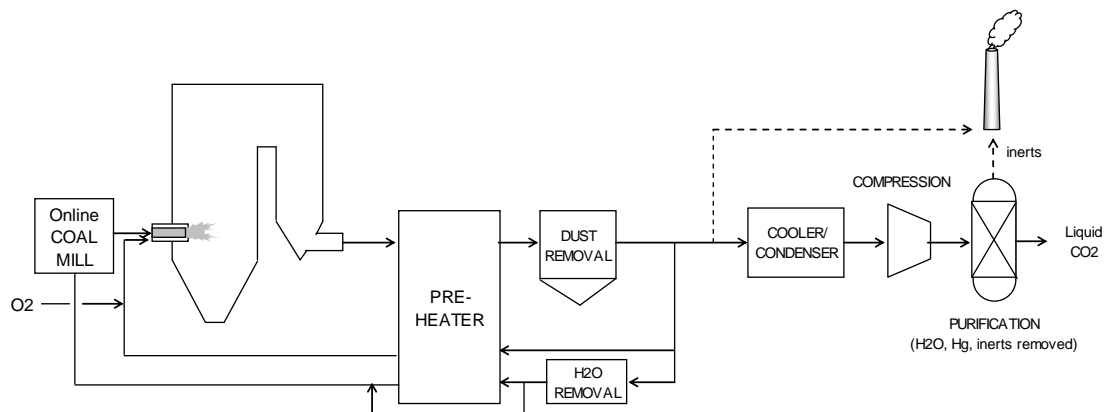


**Figure 5.** Diagram of the Callide Oxyfuel Project

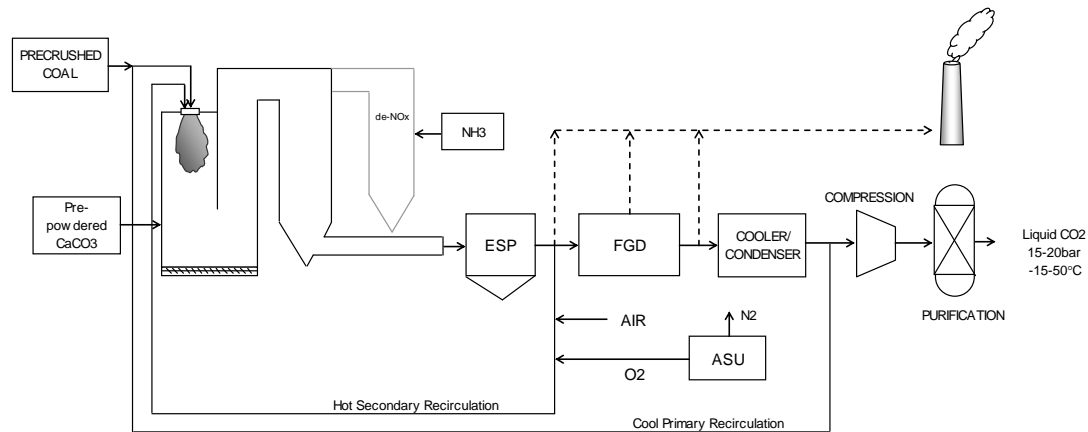


**Figure 6.** Diagram of Vattenfall's Schwarze Pumpe Oxyfuel pilot plant

#### 1.4 Flue gas impurities in oxy-fuel combustion

Oxy-fuel flue gas concentrations are determined by three factors; coal quality, process conditions and the impurity control devices that are used in the process. As  $N_2$  is not included in the oxidant and the concentration of impurities can potentially be up to 3x that of air firing for  $SO_2$  and 1.5x for  $NO_x$ . Because the flue gas is recycled, the removal of impurities downstream of the boiler will result in an overall reduction in impurity concentration within the boiler. For example, a desulfurisation unit placed inside the flue gas recycle loop would effectively reduce the  $SO_2$  concentration in the boiler to around 1.3x air firing (dependent on  $O_2$  %) and lower the downstream  $SO_2$  concentration to ~50ppm [10].

Fabric filters are expected to provide greater contact of fly ash with flue gas than ESPs for the capture of mercury species ( $Hg^0$ ,  $Hg^{2+}$ ), however the extent of capture is relative to the amount of unburned carbon, and thus also dependant on combustion conditions.

In the Schwarze Pumpe diagram (in Figure 6 above) the placement of the FGD outside of the recycle loop (for secondary flow, ~80% of total) means that the higher level of  $SO_2$  is returned to the boiler, but also allows for it to be returned at a higher temperature (increasing efficiency). A consequence of this placement is that the volume of flue gas treated by the FGD is considerably reduced, and thus could be designed as a much smaller, and less expensive unit. A consequence of the smaller unit is that under air fired operations, with a higher gas flow, poorer cleaning of sulphur gases is possible.

Clearly the optimisation of oxy-fuel circuits has a significant number of considerations (eg in a new build), however in a retrofit case, it is most likely that the existing environmental control units (or lack there of) will be retained.

While there a number of emerging commercial oxy-fuel compression processes (Air Liquide, Air Products, Linde, Praxair), a consensus is building that the boiler-side flow sheet of an oxy-fuel process is ultimately determined by Fuel-S levels [11, 12]. The Callide Oxyfuel Project will be the first demonstration of a full chain oxy-fuel process without in-line impurity control (other than a fabric filter). Instead, this process will rely on coal quality as the dominant form of controlling SO<sub>2</sub> and Hg. At the cold end (ie <200°C), the raw flue gas will use sodium polishing in a direct contact cooler followed by compression.

Figure 8 shows a diagram of the Callide compression system. The raw flue gas is conveyed to the CO<sub>2</sub> purification unit above the acid dew point (~150°C) to prevent condensation and cold end corrosion. The stream is quenched using a direct contact cooler (Scrubber 1) which lowers to gas temperature from above the acid dew point to below the H<sub>2</sub>O dew point. The quench column will also provide atmospheric scrubbing of acid gases using a caustic (NaOH/Na<sub>2</sub>CO<sub>3</sub>) wash. The gas is then compressed to 20-30bar and scrubbed (Scrubber 2) at high pressure using chilled water. The compression is expected to convert NO to water soluble NO<sub>2</sub> and potentially remove mercury. The gas is passed through absorptive dryers to remove H<sub>2</sub>O to <1ppm, before being cryogenically distilled to remove liquid CO<sub>2</sub> from the uncondensable light gases (O<sub>2</sub>, N<sub>2</sub>, Ar).

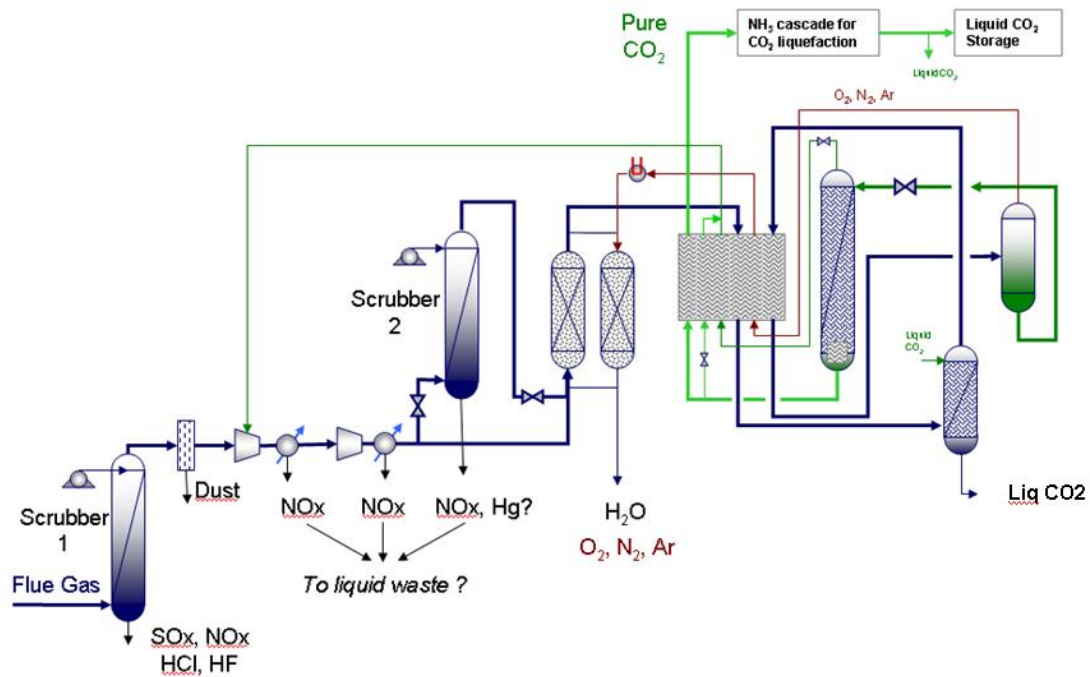


**Figure 8.** Callide Oxy-fuel compression circuit, from [13]

### 1.6 Oxy-fuel impurities during compression

Impurities in CO<sub>2</sub> have impacts in its compression. The higher concentration of SO<sub>2</sub> [14] increases the corrosion potential throughout the hot side of the plant and will ultimately produce H<sub>2</sub>SO<sub>4</sub> condensate in cooling or compression. The trace amounts of mercury can be problematic in the cryogenic heat exchangers and can be captured either in the fly ash or in the condensate. Particulates are also an issue in compression and can cause damage to compressor impellers. By comparison, NO<sub>x</sub> species are reduced (to N<sub>2</sub>) when recycled through an oxy-fuel flame and when compressed will form NO<sub>2</sub> and subsequently be absorbed in the condensate as HNO<sub>3</sub>. The greatest uncertainty in the oxy-fuel plant lies in the carry over of these impurities to the back end of the compression train where elemental mercury can form an amalgam with aluminium (which embrittles the structure) or NO<sub>x</sub>/SO<sub>x</sub> report to the CO<sub>2</sub> product (potentially corroding transport lines). Methods of removal of NO<sub>x</sub>, SO<sub>x</sub> and Hg species are commercially available and widely used in power generation, however such capture units add to the overall cost of electricity and the extent to which they are required in oxy-fuel is not certain.

The NO oxidation mechanism during compression has been observed by several oxy-fuel researchers (Air Products/Imperial College [1, 2], Linde/Vattenfall [15]).

Modelling work has suggested that the absorption mechanism will limit the capture rate to 80-85% [16]. In atmospheric conditions, NO is relatively insoluble and is oxidised slowly, however at elevated pressures this conversion process is accelerated and readily forms NO<sub>2</sub>, which is soluble in the water condensate. This mechanism forms an integral part of nitric acid production [17]. In the presence of SO<sub>2</sub>, the NO<sub>2</sub> acts as an oxidising agent forming SO<sub>3</sub> or H<sub>2</sub>SO<sub>4</sub> when in the presence of water. This reaction scheme is well known for its use in the lead chamber process, an outdated method of sulfuric acid production. In an oxy-fuel compression train this reaction mechanism is expected to enhance the absorption of SO<sub>2</sub> in the condensed water but limit NO<sub>x</sub> removal until the oxidation of SO<sub>2</sub> to SO<sub>3</sub> is complete. A complication of the lead chamber mechanism is that elemental mercury can only be captured by the condensate once HNO<sub>3</sub> begins to form. Elemental mercury is insoluble in water but may be captured as Hg(NO<sub>3</sub>)<sub>2</sub>. Figure 8 illustrates the interaction of these species. The Air Products Sour Gas Compression [18] process is the only system that actively takes advantage of the lead chamber process to remove SO<sub>x</sub>/NO<sub>x</sub> and Hg, by increasing contact time between the aqueous phase and gas phase. In other systems, such as at Callide, this mechanism is still likely to occur but to an uncertain extent.

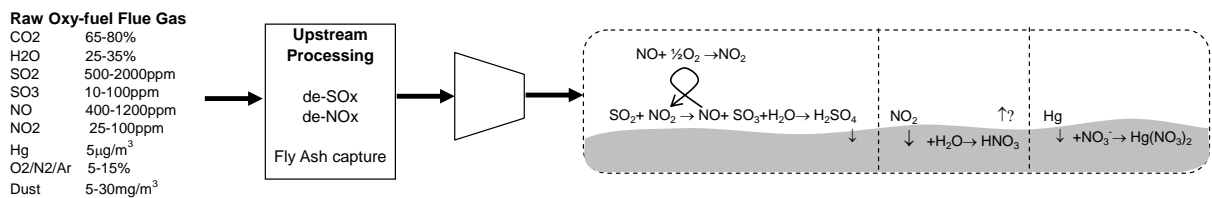


**Figure 8.** Interaction of NO<sub>x</sub>, SO<sub>x</sub> and Hg during compression of oxy-fuel flue gas

### 1.7 NO oxidation mechanisms

The oxidation process in which NO is converted to NO<sub>2</sub> and subsequently absorbed in an aqueous phase is complicated by reactions in both the gas and liquid phase. Figure 9 illustrates the potential reactions, equilibriums and species, while Figure 10 shows their relative “order of magnitude” solubilities by a comparison of the Henry’s constant at 25°C. This data is also given as Table 1 and 2 in the Appendix. Clearly the oxidation of NO to higher oxides of nitrogen enhances the absorption rate.

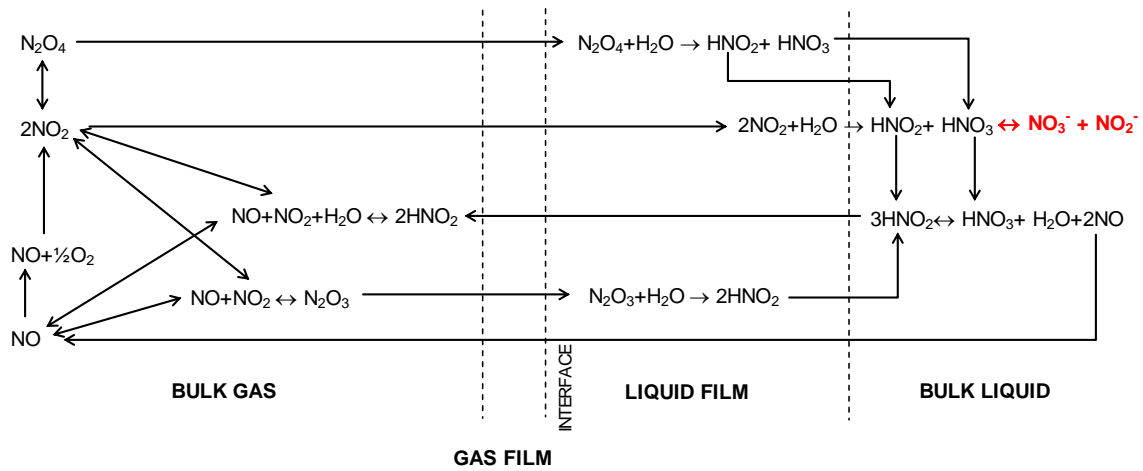


**Figure 9.**  $\text{NO}_x$  oxidation and absorption mechanisms, re-drawn from Counce and Perona [19], with added ionisation step marked in red.

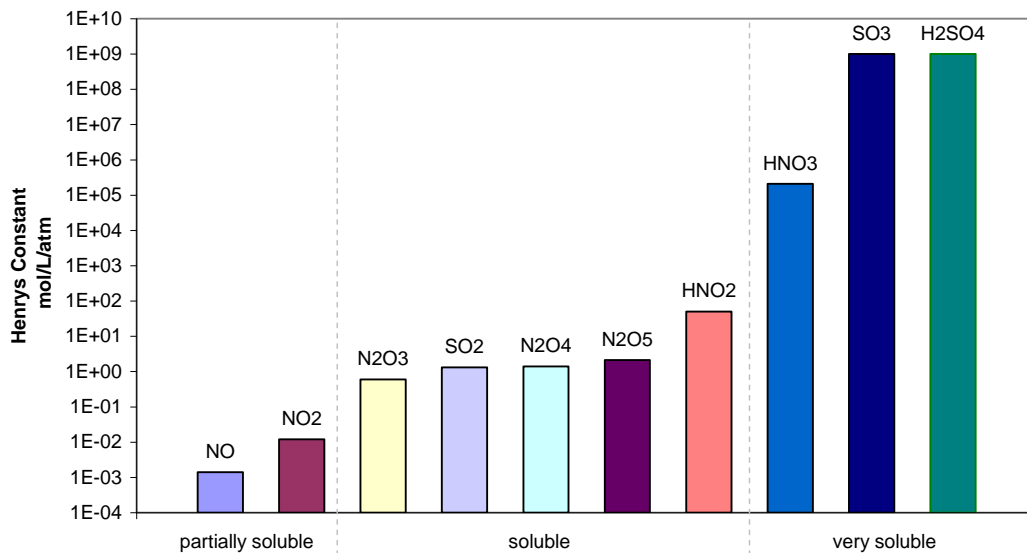
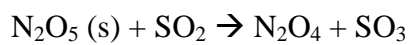
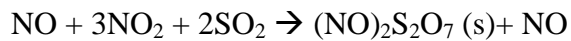
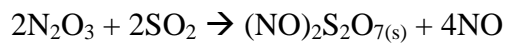
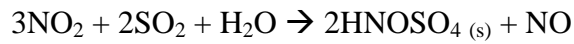


**Figure 10.** Comparison of solubilities of  $\text{NO}_x$  and  $\text{SO}_x$  gaseous species in water using Henry's Constant at 25°C (logarithmic plot, showing orders of magnitude differences). Note that  $\text{SO}_3$  and  $\text{H}_2\text{SO}_4$  values are given as infinite in [20] but expressed here as a value.

Not shown on Figure 10 is  $\text{N}_2\text{O}$ , a gas phase species with significant global warming potential which has been measured to form slowly in the presence of  $\text{NO}$  and  $\text{SO}_2$  (up to 40% of total  $\text{NO}_x$  in 3 hours [21]). It has also been shown that  $\text{NO}$  in the gas phase reacts with acid sulphate solutions forming  $\text{N}_2\text{O}$  at a rate of 20ppm/h. Such reactions were also found to be possible by recent modelling of pressurised Oxyfuel conditions [22]. Other work done on  $\text{NO}_x$  and  $\text{SO}_x$  interaction indicated the possibility of solid formation. Nelo et al. [23] observed the formation of a white solid when reacting  $\text{SO}_2$

and NO in the presence of ozone under wet conditions. The solid was theorised to be a mixture containing  $(\text{NO}_2)_2\text{S}_2\text{O}_7$  and  $\text{HNOSO}_4$  [23] and potentially  $\text{N}_2\text{O}_5$  (in  $\text{NO}_x$  only systems) which is solid at room temperature. They also found that a significant difference between the change in gaseous  $\text{NO}_x$  concentration and the amount of nitric acid in solution. The theoretical reactions for this process are:



Recent work done at the Technical University of Hamburg [24] also indicated the formation of white solids in their laboratory oxy-fuel drop tube furnace and compression plant, though no chemical identification has yet been published.

## **2. Project objectives**

*The objective is to establish the feasibility of CO<sub>2</sub> gas quality control in oxy-fuel technology by removal of sulfur oxide and nitrogen oxide gas impurities during compression from condensed moisture in the flue gas as liquid acids.*

The method proposed for assessing the feasibility for the clean up is to build an experimental rig for testing of CO<sub>2</sub> compression, and undertaking laboratory experiments on the impurities

The focussing questions for the experiments are based on the mechanisms by which the impurities are expected to be removed, namely:

- *What is **the extent of oxidation of the insoluble primary nitrogen oxide - NO - in flue gas to soluble NO<sub>2</sub> during compression?***
- *What is the possibility of **interference of the nitrogen chemistry to form NO<sub>2</sub> by SO<sub>2</sub>?***
- *Are sulphur gases absorbed to form a liquid acid – H<sub>2</sub>SO<sub>4</sub> - in addition to HNO<sub>3</sub>?*
- *Is SO<sub>x</sub> absorption catalysed by the formation of higher nitrogen oxides, in particular NO<sub>2</sub>, and does it occur in the gas or aqueous phase?*

### **3. Experimental**

#### *3.1 Apparatus*

The challenge in this study involved the need to contact  $\text{NO}_x$  and  $\text{SO}_x$  gases with water at pressures up to 30bar. A 300mL stainless steel (304) vessel with a corrosion resistant sulfinert coating was used as the contactor, with gas mixtures introduced through a central stem that extended into 150mL of water creating a bubbling interface. This system uses a continuous gas/batch liquid process. While the use of this system created an “uncontrolled” and “undefined” interfacial area of contact between gas and liquid, it does provide good gas/liquid contact and also introduces turbulent mixing to avoid mass transfer effects. The experimental apparatus is shown in Figure 11. The bypass line was used during set-up to adjust the flow rates of  $\text{N}_2$ ,  $\text{O}_2$  and  $\text{NO}$  (diluted from a 1% mix of  $\text{NO}$  in  $\text{N}_2$ ). It was found in practice that simply setting the Mass Flow Controllers (MFC's ) and dialling up the pressure resulted in significant changes to flow rates and thus gas concentrations. To maintain the same gas flows under all pressures, a Honeywell mass flow meter (AWM5000 0-5L/min) was connected to the exhaust prior to the experiment (operating in bypass) and the flows were matched after the pressure was set. This mass flow meter worked on the same principal as mass flow controllers, sensing mass flow through heat transfer to the incoming gas. This flow meter was removed during the experiment to avoid corrosion in the wet environment. Pressure was set using the back pressure regulator and gas concentrations were measured using a Testo 350XL Flue Gas Analyser. The Testo unit sampled approximately 1.4L/min from the exhaust line and measured  $\text{O}_2$ ,  $\text{NO}$ ,  $\text{NO}_2$  and  $\text{SO}_2$  using electrochemical cells. The output of these cells are internally weighted for interactive effects of other gases and logged continuously per second using the Testo software. Long term measurements at high gas concentrations can cause electrochemical cells to become saturated and necessitate recharging, however rinsing was performed after the experiment with no operational effects.

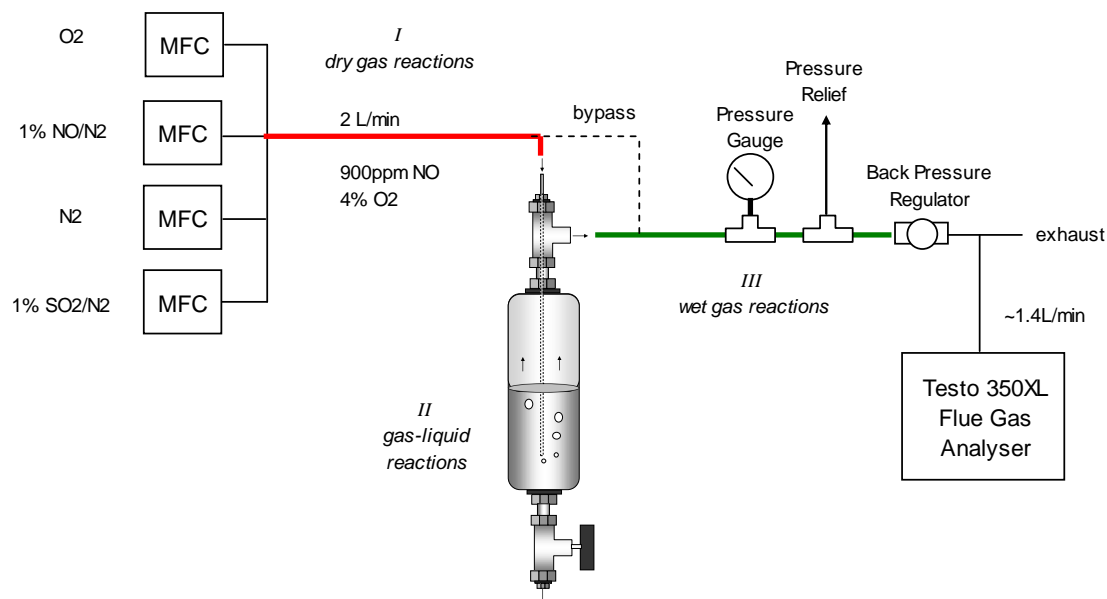


**Figure 11.** Pressurised laboratory apparatus for contacting  $\text{NO}_x$  gases with water, indicating the three different conditions for reactions involving I - dry gas, II – gas-liquid and III – wet gas

### 3.2 Experiments

Experiments were performed using a nominal 900ppm NO mixture in 4%  $\text{O}_2$ , with the balance being  $\text{N}_2$ . In practice the starting concentration varied by  $\pm 50$ ppm due to the resolution in the MFC's and in the flow meter. The reactor and transport lines include three potential conditions for  $\text{NO}_x$  reactions to take place; dry gas phase reactions (I), gas-liquid contacting reactions (II) and wet gas phase reaction (III).

This report covers experiments undertaken to study the dry gas phase reactions (I, with no liquid in the reactor) and experiments involving (I+II+III, with liquid in the reactor) to determine the maximum impact of pressure on NO oxidation at room temperature.

**Dry experiments** (without the presence of water) were performed with and without the reactor to identify the effects of gas kinetics, in particular the conversion occurring within the transport lines.

**Wet experiments** were performed by contacting the gas for 10 minutes with continuous gas analysis, and then comparing the captured  $\text{NO}_x$  with that of the liquid phase  $\text{NO}_x$ . Several experiments were conducted over 8 hour continuous operation with gas measurement to provide a “pseudo-equilibrium” comparison. A suite of experiments have been also performed using a mixed 1000ppm  $\text{SO}_2$ /1000ppm NO feed gas, however the gas analysis technique appears to have interference between  $\text{SO}_2$  and  $\text{NO}_2$ . Therefore only the liquid analysis is presented here.

## 4. Results

### 4.1 Dry $\text{NO}_x$ System

Increasing pressure in the dry  $\text{NO}_x$  system had a pronounced effect on the oxidation of NO, readily producing  $\text{NO}_2$ . Figure 12 shows this influence under a constant flow of 2 L/min (at room temperature and atmospheric pressure). This majority of this conversion occurred below 10 bar. The constant total  $\text{NO}_x$  indicates that no other significant species are formed. An important point with this system (and any oxy-fuel compression system) is that the flow rate is not constant within the reactor. Every sequential pressure increase reduces the volumetric flow and hence also increases residence time. By way of example the residence time inside the reactor is 12.3 seconds at ambient pressure but increases to 254.2 seconds at 20 bar. Figure 13 compares the conversion of NO to  $\text{NO}_2$  with and without the reactor connected. It can be observed that significant conversion occurs inside the transport lines despite making up only 17% of the residence time. Figure 14 compares the experimental results of the NO oxidation with the global kinetic reaction recommended by Tsukahara et al[25] and used by LINDE [26]. Details of this reaction are given in the Appendix. The experimental results are considered as Reactor Only (which subtracts the effects of the transport lines, shown in Figure 13) and the total conversion within the apparatus. As can be observed, the global mechanism provides an excellent prediction of results over a wide range of pressures and residence time.

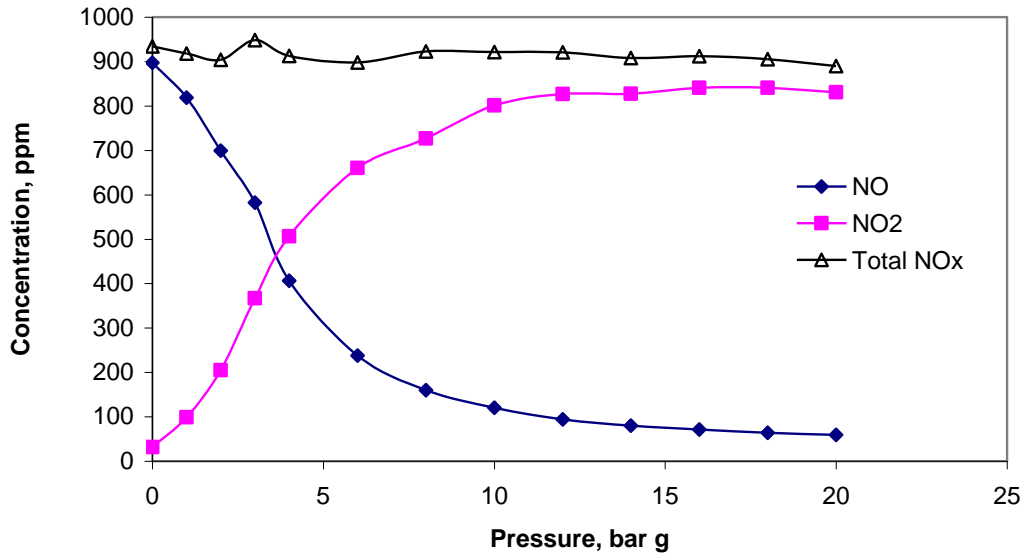


**Figure 12.** Effect of pressure on the oxidation of NO to NO<sub>2</sub> (in 4% O<sub>2</sub>) without water. The points in this figure and Figures 13 to 16 correspond to results for individual experiments at a number of pressures for common periods of 10 minutes.

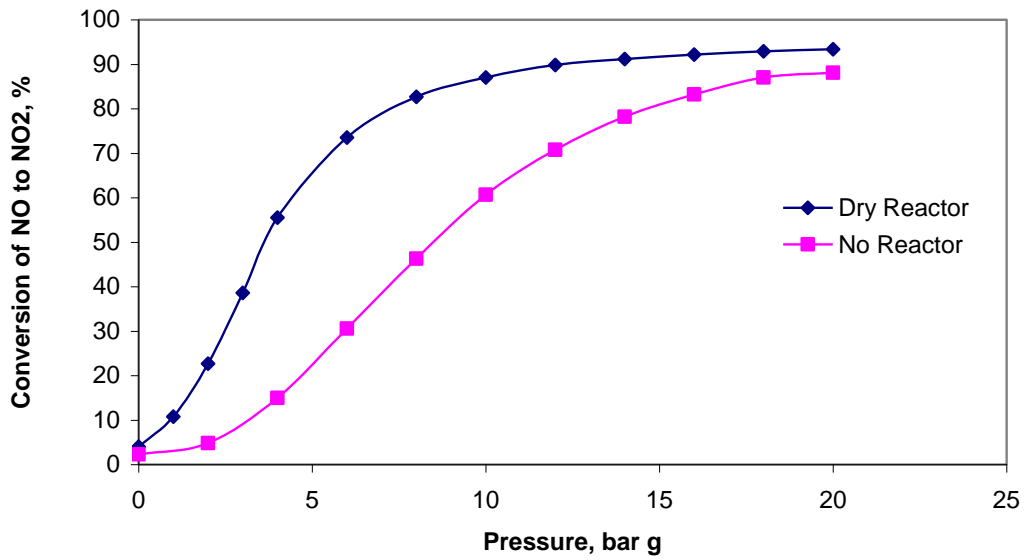


**Figure 13.** Comparison of NO<sub>x</sub> conversion in reactor and transport lines showing effect of residence time

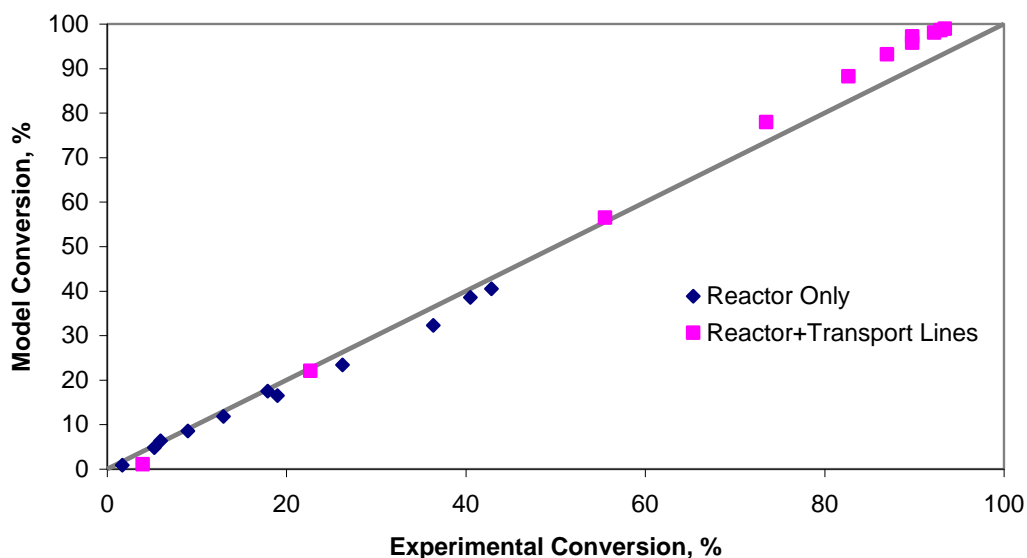


**Figure 14.** Evaluation of global kinetic model detailed in the Appendix to measured experimental results, with results for two differing durations corresponding to residence times in the reactor only, and the reactor with transport lines

#### 4.2 Wet $\text{NO}_x$ System

The wet  $\text{NO}_x$  system provided significantly different results from the dry  $\text{NO}_x$  experiments. Figure 15 shows the gas concentrations of  $\text{NO}$  and  $\text{NO}_2$  after contacting the water for 10 minutes. Marked in grey are the dry  $\text{NO}_x$  results for comparison. The  $\text{NO}$  does not appear to be affected by the presence of water, however there is a significant reduction in  $\text{NO}_2$ . These gas concentrations did not appear to vary greatly with time, even after 8 hours in the pseudo-equilibrium experiments. The aqueous  $\text{NO}_x$  species are shown in Figure 16, along with the 8 hours results. The amount of  $\text{NO}_3^-$  makes up the dominant species in the water, however there was still a significant amount of  $\text{NO}_2^-$  present considering that nitrite (as  $\text{HNO}_2$ ) is 5 orders of magnitude less soluble than nitrate (as  $\text{HNO}_3$ ). The “equilibrium” results taken at 1, 10 and 20 bars reveal that the absorption of nitrate,  $\text{NO}_3^-$ , has reached ~50% of its absorption capacity in 10 minutes. The final pH of the water after 10 minutes varied from 4 at ambient pressure to 2.75 at 30 bars. By comparison, the equilibrium experiments gave a final pH of ~0.76-0.71 for pressures 10 and 20 bars, respectively. Overall, it was found that the amount of  $\text{NO}_3^-/\text{NO}_2^-$  and  $\text{HNO}_2$  (estimated from equilibrium) present in the water could only account for 15-22% of the total  $\text{NO}_x$  that appears to be captured from gas stream. It is postulated that the unaccounted  $\text{NO}_x$  species in the gas is present as

gaseous  $\text{HNO}_3/\text{HNO}_2$  which is not expected to be measured in the Testo flue gas analyser.

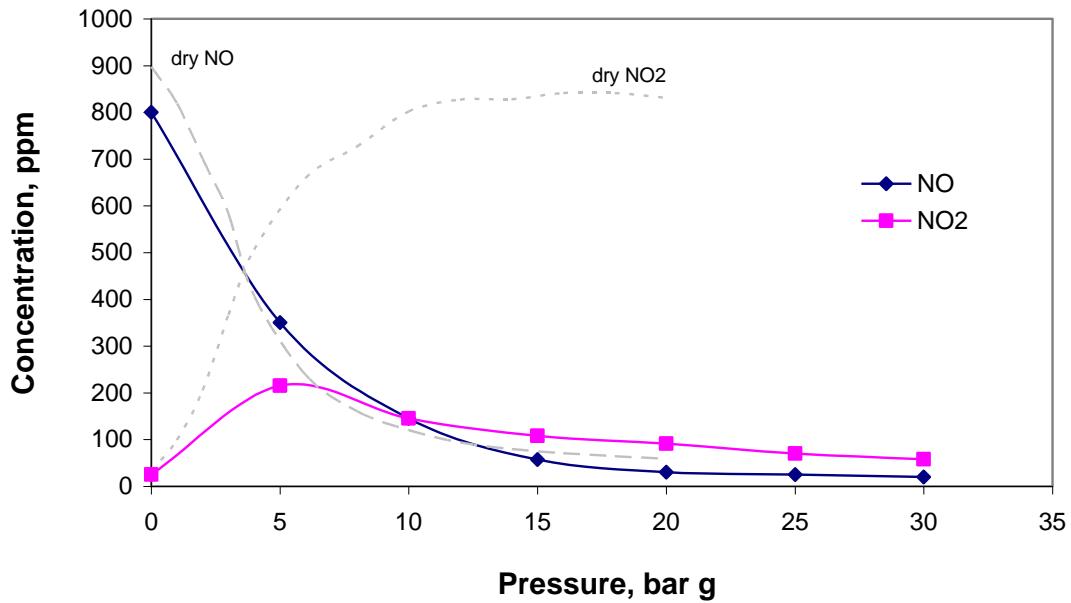


**Figure 15.** Gaseous  $\text{NO}_x$  concentrations after contacting water at different pressures. Lines in grey compare the dry experimental results

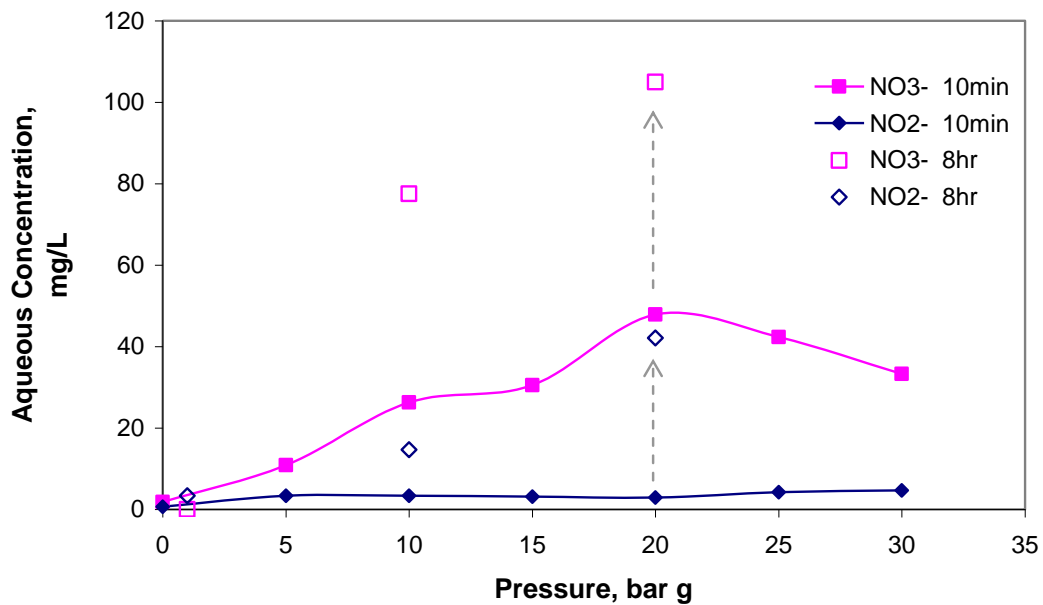


**Figure 16.** Aqueous  $\text{NO}_x$  species present in the water after continuous contact with the gas stream for either 10 minutes or 8 hr “pseudo-equilibrium” conditions.

#### 4.3 Wet $\text{SO}_x/\text{NO}_x$ system

The mixed feed gas consisting of 1000ppm  $\text{SO}_2$  and 1000ppm  $\text{NO}$  was fed into the wet contacting system with both continuous gas and batch liquid analyses being performed. Interference between  $\text{SO}_2$  and  $\text{NO}_2$  caused the Testo to give a zero  $\text{NO}_2$  reading and it

is not yet clear if this was a false signal. Figure 17 gives the liquid analysis for this set of results. These also show non-uniform trends. At ambient pressure, the amount of  $\text{SO}_4^{2-}$  is considerably higher than other species, but appears to drop in concentration as pressure increases. At 20 bar the amount of  $\text{SO}_4^{2-}$  begins to increase once again, though not to the extent of  $\text{SO}_3^{2-}$ . By comparison, the  $\text{NO}_3^-$  also shows a significant concentration at ambient conditions. At pressures of 5-15bar, the  $\text{NO}_3^-$  concentration closely follows the results of the Wet  $\text{NO}_x$  only system (ie without  $\text{SO}_2$ ) and at 20 bar this concentration drops to  $\sim 2\text{mg/L}$ . The concentration of  $\text{NO}_2^-$  closely matches the results from the Wet  $\text{NO}_x$  system for all pressures except 20bar, where it is also reduced to zero. It is clear from the mixed gas system that the  $\text{NO}_x$  absorption is higher at pressures of 5-15 bar g, while  $\text{SO}_x$  absorption is higher at ambient pressure and 20bar. The transition from  $\text{SO}_4^{2-}$  to  $\text{SO}_3^{2-}$  is significant at 20 bar because the concentrations of  $\text{NO}_2^-$  and  $\text{NO}_3^-$  both decrease, indicating that interaction between species is occurring. It is clear that this is a complex system, which involves both gas and liquid mechanisms. Further work should be undertaken to overcome the issues associated with the gas analysis and a mechanistic approach to this complex system needs to be adopted. Future experiments will introduce  $\text{H}_2\text{O}$  in the gas phase only and study  $\text{SO}_2$  absorption without  $\text{NO}_x$ .

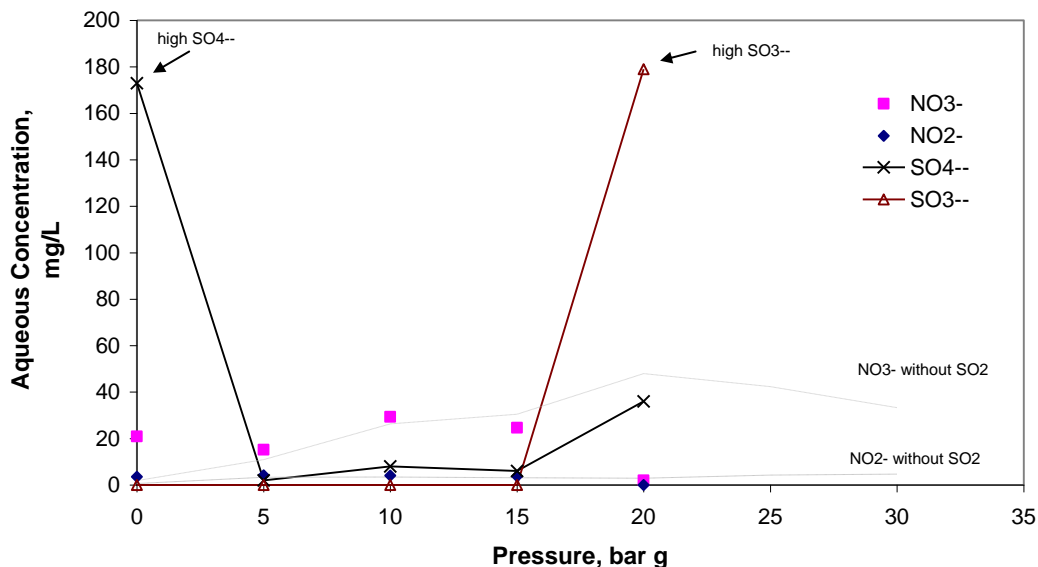


**Figure 17.** Aqueous  $\text{NO}_x$  and  $\text{SO}_x$  species present in solution after 10 minutes contact time (feed gas mix 1000ppm  $\text{SO}_2$ , 1000ppm  $\text{NO}$ , 3.5%  $\text{O}_2$ ,  $\text{N}_2$  balance). Lines marked in grey are results for  $\text{NO}_x$  only contacting.

#### 4.4 Thermodynamics

The thermodynamics package FACTSage was used to model equilibrium conditions in the wet and dry pressurised system. In practice it was found that almost all  $\text{NO}_x$  species converts to  $\text{N}_2$  under equilibrium conditions, however given that this does not reflect reality, the  $\text{N}_2$  species was excluded from the equilibrium calculations. The dry  $\text{NO}_x$  system results are given in Figure 18, with  $\text{NO}_2$  as the dominant  $\text{NO}_x$  species formed. Lesser amounts of  $\text{N}_2\text{O}$  are formed at pressures lower than 6 bar while this reaction is suppressed at higher pressures by the formation of  $\text{N}_2\text{O}_4$ . Other species, such as  $\text{NO}$  are formed at concentrations lower than 1ppm and are not considered significant across the entire pressure range. Comparison to the dry experimental results indicates that the measured results operate under kinetically limited conditions. The Testo manufacturer suggests that the flue gas analyser is very likely to include  $\text{N}_2\text{O}_4$  species in the  $\text{NO}_2$  electrochemical cell (counting as  $2\text{NO}_2$ ). However, this does not appear to have an effect on the dry kinetic modelling in Figure 14.

The equilibrium modelling of the wet  $\text{NO}_x$  system provided a greater number of species. A  $\text{H}_2\text{O}$  content of 20% was used to simulate the excess water in a real system, though it should be noted that the effect of pressure caused a mild increase in  $\text{H}_2\text{O}$  condensation. Figures 19 and 20 give the equilibrium results for gas and aqueous phase. These figures have been placed on a logarithmic scale to show the order of magnitude differences between species. Pressure did have an influence on both sets of results, however the pressure effect is small compared to the significant differences in species concentrations. In the gas phase,  $\text{HNO}_3$  is the dominant species, followed closely by  $\text{NO}_2$ . Both concentrations are much less than 1ppm. These gases are matched in the aqueous phase by  $\text{NO}_3^-$  and  $\text{HNO}_3$  (present in water in its molecular phase). Of particular interest is the presence of  $\text{HNO}_2$  in the gas phase and  $\text{NO}_2^-/\text{HNO}_2$  in the liquid phase. These species concentrations are orders of magnitude below the dominant  $\text{NO}_x$  species, however, the analysis of the water after 10 minutes of  $\text{NO}_x$  gas contact shows the presence of  $\text{NO}_2^-$  in measurable quantities. Similar amounts of  $\text{NO}_3^-/\text{NO}_2^-$  were observed on Linde's compression train at Schwarze Pumpe [15].

Given that the equilibrium partition between  $\text{HNO}_2$  in and  $\text{NO}_2^-$  in the liquid favours the molecular form (from Figure 20), it is considered that  $\text{HNO}_2$  may also be present in significant amounts in the gas phase. In the reaction scheme proposed by Winkler et al

[26],  $\text{HNO}_2$  and  $\text{HNO}_3$  are present in the liquid, but convert to  $\text{N}_2\text{O}_3$ ,  $\text{N}_2\text{O}_4$ ,  $\text{NO}$  and  $\text{NO}_2$  in the gas phase.

Earlier modelling work by Counce and Perona [19], (shown in Figure 9) considered  $\text{HNO}_2$  as a species which could potentially desorb from the bulk liquid given its substantial vapour pressure. However they also considered it as a species which decomposed at ambient conditions to form  $\text{NO}$ ,  $\text{NO}_2$  and  $\text{H}_2\text{O}$ . By contrast,  $\text{HNO}_3$  was not considered an important gas phase species due to its low vapour pressure. These insights are important given that most work with  $\text{NO}_x$  absorption is for ambient pressures and temperatures (ie, atmospheric modelling, medical  $\text{NO}_x$ ), and do not consider a cryogenic stage downstream.

Despite the low gas concentration of  $\text{HNO}_3$  and even lower concentration for  $\text{HNO}_2$  in the thermodynamic model of this report, the results clearly favour the formation of  $\text{HNO}_3$  over  $\text{NO}_2$  and  $\text{HNO}_2$  over  $\text{NO}/\text{N}_2\text{O}_3/\text{N}_2\text{O}_4$  in the gas phase.

While the work presented here is ongoing, it does raise some fundamental implications for downstream processing during compression of oxy-fuel flue gas. In particular, where a carry over of  $\text{HNO}_2$  may report to and when it may decompose to form  $\text{NO}/\text{NO}_2/\text{H}_2\text{O}$ .

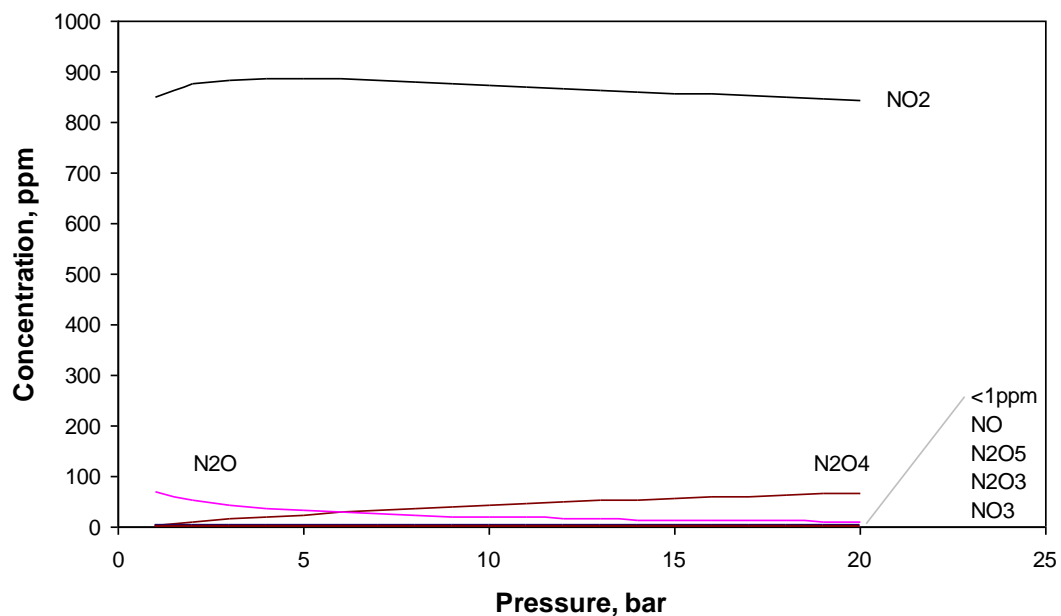


**Figure 18.** Thermodynamic modelling of dry  $\text{NO}_x$  system using FACTSage at  $25^\circ\text{C}$  (1000ppm  $\text{NO}$ , 3%  $\text{O}_2$ , balance  $\text{CO}_2$  starting)

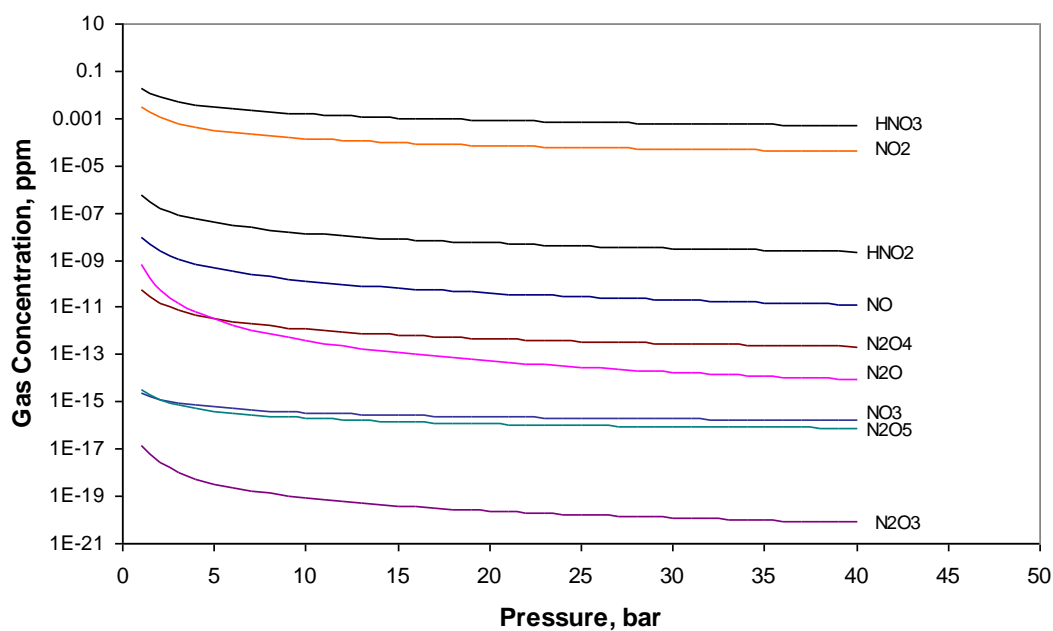


**Figure 19.** Thermodynamic modelling of gas species in wet NO<sub>x</sub> system using FACTSage at 25°C (1000ppm, NO, 20% H<sub>2</sub>O, 3% O<sub>2</sub>, balance CO<sub>2</sub> starting)

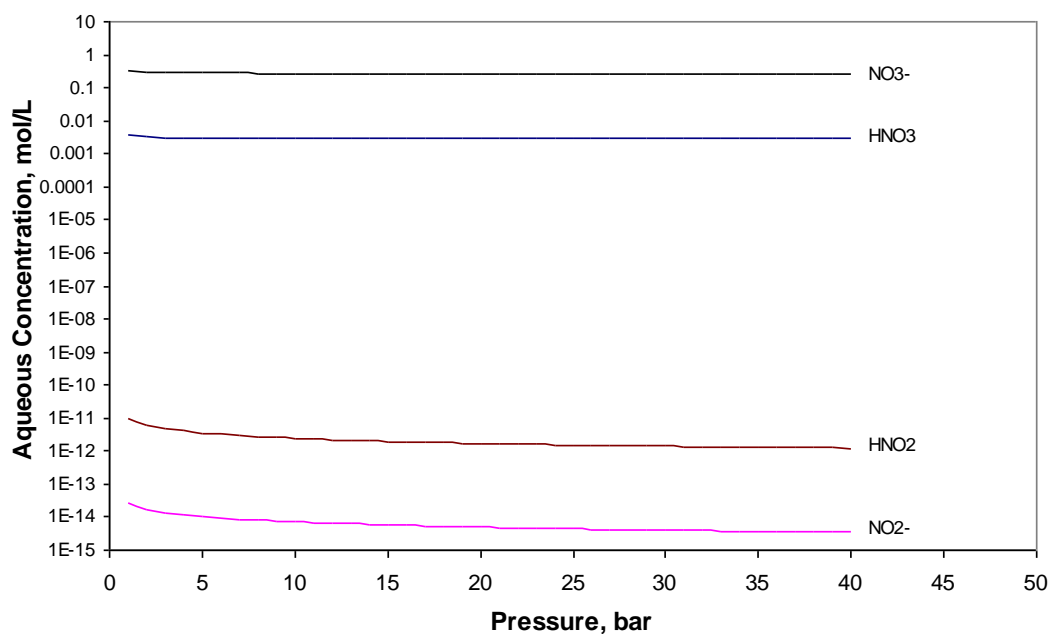


**Figure 20.** Thermodynamic modelling of aqueous species in wet NO<sub>x</sub> system using FACTSage at 25°C (1000ppm NO, 20% H<sub>2</sub>O, 3% O<sub>2</sub> starting)

#### 4.6 Final comments

The behaviour of NO<sub>x</sub> in dry and wet pressurised conditions (up to 30 bar) indicates that dry NO oxidation can be readily predicted using a simple global reaction (detailed in the Appendix). The wet NO<sub>x</sub> system (continuous gas flowing through a bubbling

batch liquid phase) gave significantly different results, enhancing the absorption of  $\text{NO}_2$  from the gas phase and favouring the production of nitrate ions ( $\text{NO}_3^-$ ) in the liquid phase as pressures were increased. The presence of nitrite ions ( $\text{NO}_2^-$ ) were considered to reflect the larger amount of molecular  $\text{HNO}_2$  in the liquid phase. Pseudo-equilibrium experiments suggested that approximately 45% of the nitrate formation occurred in the first 10 minutes of gas-liquid contact, while the formation of nitrite was considerably slower (7%). Thermodynamic modelling was used to evaluate equilibrium conditions for compressing oxy-fuel flue gas and found that almost 100% of gaseous  $\text{NO}_x$  species were captured in the liquid phase as nitrate ions. Of the remaining gas phase, the dominant  $\text{NO}_x$  species was  $\text{HNO}_3$ . The amount of nitrite ions measured in the liquid phase was not predicted by thermodynamics.

Closing the mass balance over the wet experiments on the nitrogen element for the analysed gases and liquids has proven to be difficult due to the potential formation of a number of secondary species, most of which are not readily analysed.

Pires and Rossi [21] showed that a mixed feed gas with  $\text{NO}$  and  $\text{SO}_2$  will form a significant amount of  $\text{N}_2\text{O}$  as the pH of the liquid becomes highly acidic (ie  $\text{pH} < 3$ ). Pettersson et al [22] used the Pires and Rossi mechanism to model  $\text{N}_2\text{O}$  formed in pressurised Oxyfuel conditions along with the formation of acid condensates. Their results indicated that  $\text{NO}_3^-$  concentration reached around 7500mg/L at 20bar in 100seconds contact time. This is comparable to measured oxy-fuel compression condensates of 4900mg/L  $\text{NO}_3^-$  by Keopke et al [24]. In this work, the maximum  $\text{NO}_3^-$  concentration measured was 105mg/L during the 8 hour pseudo-equilibrium conditions at 20bar (without  $\text{SO}_2$  present). Such an order of magnitude difference between the current and literature results suggests that the contact surface area inside a oxy-fuel compression system may be considerably higher than within the laboratory bubble column. In the Callide system such gas-liquid contact may occur through mist formation after each compression stage, wetted wall contact at the intercoolers and in the packed column at the final stage of high pressure  $\text{NO}_x$  absorption.

Candidate secondary species include  $\text{HNO}_2$  (which dissociates back to  $\text{NO}$  and  $\text{NO}_2$ ) or  $\text{N}_2\text{O}_5$  (a white solid at room temperature which can dissociate to  $\text{NO}_2$  and  $\text{O}_2$ ). With

the addition of SO<sub>2</sub> the list of potential “candidate” secondary species include N<sub>2</sub>O, (NO)<sub>2</sub>S<sub>2</sub>O<sub>7</sub> and HNOSO<sub>4</sub>.

## **5. Future Work**

The experiments have shown that interpretation of the dry gas phase conditions are relatively simple, while mixed conditions (ie dry gas/gas-liquid contact/wet gas) create a very complex system with similarly complex results.

Future work should focus on several areas:

- *Separation of the three experimental conditions identified on Figure 11 to study the effect of wet gas phase only and gas-liquid contacting only* – these experiments will aid in determining which species are currently being lost to the analysis and the extent of their impact. Such work is currently underway using a bubbling system to pre-saturate the N<sub>2</sub> prior to mixing the gases. Tests will also include removing O<sub>2</sub> to see the effect of H<sub>2</sub>O vapour only. The current experiments have been conducted in an N<sub>2</sub> atmosphere, additional experiments in CO<sub>2</sub> should be made, as this represents the real oxyfuel flue gas.
- *Conduct comparative experiments with SO<sub>2</sub> only (ie no NO<sub>x</sub>)-* determining whether the NO oxidation process is enhancing/catalysing the absorption of SO<sub>2</sub> requires a baseline for comparison. The work conducted here has shown that the effects of a mixed gas system produce results that lack a definitive trend and this may be because of multiple mechanisms occurring. Future work will focus on lower SO<sub>2</sub> concentrations as expected in the Callide Oxyfuel Project
- *Studying Hg removal by addition of gaseous Hg to feed gas* – adding Hg to the experiment represents a significant challenge, more so in high pressure system. The current plans are for Hg addition to occur by bubbling Hg laden gas through controlled HNO<sub>3</sub> solutions to compare capture performance without the complexity of NO gas-liquid mechanisms. Further work in a mixed feed gas systems will be dependant on the results of the controlled solution test.
- *Identification of NO<sub>x</sub> species* –an important aspect of future work is to identify the solubility of the N<sub>x</sub>O<sub>y</sub> products. It is beyond the scope of this project and

laboratory capability to perform measurements for each of the many potential individual species. This would require on-line and high pressure FTIR gas phase analysis having a high cost, which is not currently considered justifiable. Instead, the focus will be on whether the  $N_xO_y$  species formed are soluble and form liquids. The effort will therefore focus on the analysis of the liquid products. Experiments could be performed using a high pressure caustic wash to capture any soluble gas phase  $NO_x$  species exiting the main bubbling apparatus. This work could be supported by FTIR analysis on batch gas samples and a wider thermodynamic study in different conditions.

- *Incorporation of condensing moisture* - in practice as pressure increases flue gas moisture will condense as a mist of high surface area, and hence high reactivity for acid formation from acid gases. A compression system to facilitate mist formation is planned for a later part of the project.

## **6. Conclusions**

Experiments involving the pressurised contacting of gaseous  $NO_x$  and  $SO_x$  with liquid water were undertaken using a custom built apparatus. The gases were bubbled through a set amount of water with gas analysis being measured continuously during the experiment and the liquid analyses taken at the end.

The experiments have established the feasibility of  $CO_2$  gas quality control in oxy-fuel technology by removal of sulfur oxide and nitrogen oxide gas impurities during compression as liquid acids.

The findings are summarised according to the focussing questions:

*Extent of NO oxidation during compression* – it was found that insoluble NO readily oxidized to soluble  $NO_2$  with increasing pressure under dry conditions. The conversion rate was found to exceed 90% above a pressure of 15 bar. This oxidation was found to

be kinetically limited and could be predicted using a single global reaction scheme (see Appendix).

**Practical implications:** the extent to which NO is oxidized in an oxy-fuel compression train will depend on the residence time and pressure within each compression stage. Given that the final pressure during processing will exceed 20bar, an overall conversion exceeding 93 % can be expected. This suggests that there is a significant opportunity to remove NO<sub>x</sub> impurities during oxy-fuel CO<sub>2</sub> purification.

*Absorption of NO<sub>2</sub> to form nitric acid as a condensate* – the wet contacting experiment showed that 97% of the feed NO could be removed at 30 bar and that the NO<sub>x</sub> gases exiting the system was less than 100ppm. An increase of pressure resulted in an increased formation of nitrate in the liquid product, NO<sub>3</sub><sup>-</sup>, with reduced amounts of nitrite, NO<sub>2</sub><sup>-</sup>. Above a pressure of 20 bar the extent of nitrate ions was reduced in favour of nitrite ions. However, in attempting to close the mass balance between gaseous and aqueous NO<sub>x</sub> a significant amount of gaseous NO<sub>x</sub> has been unaccounted for. It is suggested that this is due to the available gas analysis methods being unable to analyse higher order N<sub>x</sub>O<sub>y</sub> species expected from a thermodynamic assessment.

**Practical implications:** the saturated conditions and pressures in an oxyfuel compression circuit suggest that a significant conversion of NO to higher order oxides can be expected. Such oxides are more soluble than either NO or NO<sub>2</sub> and thus would most likely react with the condensate to form liquid acids. In previous studies there is some evidence of white solid N<sub>x</sub>S<sub>y</sub>O<sub>z</sub> formation in laboratory oxy-fuel compression systems and in NO oxidation studies. The solid could potentially cause blockages in areas downstream of any water removal stages (ie if no liquid water is present).

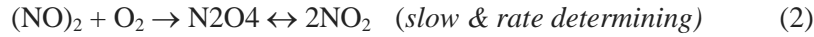
*Absorption of SO<sub>2</sub> and interference with NO<sub>x</sub> oxidation-* the experiments have shown that SO<sub>2</sub> is absorbed in the liquid as either H<sub>2</sub>SO<sub>4</sub> or H<sub>2</sub>SO<sub>3</sub>. At a pressure of 20bar, the SO<sub>2</sub> absorption in the liquid had a significantly negative effect on NO<sub>x</sub> absorption. At the intermediate pressures 5-15bar, NO<sub>x</sub> remained unaffected (ie similar to results without the presence of SO<sub>2</sub>) and the absorption of SO<sub>2</sub> was not significant.

**Practical implications:** During multi-stage CO<sub>2</sub> compression it is most likely that remaining SO<sub>2</sub> will be removed during early stages along with the majority of the water vapour. At pressures above 20bar, NO<sub>x</sub> oxidation and absorption to form acid may not be restricted by the existence of SO<sub>x</sub>.

## Appendix

### Global Reaction of NO Oxidation

According to Joshi and co-workers [27], nitric oxide (NO) is oxidized in 2 steps, initially forming an intermediate dimer (NO)<sub>2</sub> in a fast reaction followed by a slower oxidation step with O<sub>2</sub>. However, below 350°C, the back reaction is negligible



Reaction (1) is in equilibrium with a equilibrium constant of

$$K_e = [(\text{NO})_2]/[\text{NO}]^2 \quad (3)$$

The oxidation rate of NO can be shown to be

$$\text{Rate} = k[(\text{NO})_2][\text{O}_2] \quad (4)$$

$$= kK_e[\text{NO}]^2[\text{O}_2] \quad (5)$$

$$= k_c[\text{NO}]^2[\text{O}_2] \quad (6)$$

In this case the approximation of  $kK_e$  as  $k_c$  simplifies the overall reaction scheme to a global reaction and produces a negative activation energy (due to the inclusion of the equilibrium constant). The effect of this produces a higher rate at lower temperatures. Tsukahara et al [25] summarised a number of kinetic studies and recommended this global reaction to be



With the reaction rate given as

$$\frac{d[\text{NO}_2]}{dt} = 2400 \exp\left(\frac{530}{T}\right) [\text{NO}]^2 [\text{O}_2] \quad (8)$$

This reaction form has been used previously by Linde as part of their pilot ‘‘Cold DeNOx’’ work [26] with compressed oxy-fuel flue gas.

**TABLE 1. Reactions and Equilibrium values for Counce and Perona NOx mechanisms [19]**

Reaction/equilibrium	Rate constant	K eq	Source
2NO + O <sub>2</sub> = 2NO <sub>2</sub>	k = 2400exp(530/T)		[28]
2NO <sub>2</sub> = N <sub>2</sub> O <sub>4</sub>		6.86	[29]
NO + NO <sub>2</sub> = N <sub>2</sub> O <sub>3</sub>		0.535	[29]
NO + NO <sub>2</sub> + H <sub>2</sub> O = 2HNO <sub>2</sub>		0.0531	[29]
2NO <sub>2</sub> + H <sub>2</sub> O = HNO <sub>2</sub> + HNO <sub>3</sub>	k = 7E7		[21]
N <sub>2</sub> O <sub>4</sub> = H <sub>2</sub> O = HNO <sub>2</sub> + HNO <sub>3</sub>	k = exp(16.38-3163/T)		[30]
HNO <sub>2</sub> = H <sup>+</sup> + NO <sub>2</sub> <sup>-</sup>		5.1E-4	[29]
HNO <sub>3</sub> = H <sup>+</sup> + NO <sub>3</sub> <sup>-</sup>		15.4	[29]

**TABLE 2. Solubility values for NO<sub>x</sub> and SO<sub>x</sub> species [20] at 25°C****NO<sub>x</sub> species**

Substance	Henry's Constant [M/atm]	Original source
Nitric oxide, NO	$1.4 \times 10^{-3}$	Lide and Frederikse (1995)
Nitrogen dioxide, NO <sub>2</sub>	$1.2 \times 10^{-2}$	Chameides (1984)
Dinitrogen trioxide, N <sub>2</sub> O <sub>3</sub>	$6.0 \times 10^{-1}$ $2.6 \times 10^{-1}$	Schwartz and White (1981) Durham et al. (1981)
Dinitrogen tetroxide, N <sub>2</sub> O <sub>4</sub>	1.4 1.6	Schwartz and White (1981) Durham et al. (1981)
Dinitrogen pentaoxide, N <sub>2</sub> O <sub>5</sub>	2.1	Fried et al. (1994)
Nitrous acid, HNO <sub>2</sub>	50	Becker et al. (1996)
Nitric acid, HNO <sub>3</sub>	$2.1 \times 10^5$	Lelieveld and Crutzen (1991)

**SO<sub>x</sub> species**

Substance	Henry's Constant [M/atm]	Original source
Sulfur dioxide, SO <sub>2</sub>	1.3	Kavanaugh and Trussell (1980)
Sulfur trioxide, SO <sub>3</sub>	Infinity	Sander and Crutzen (1996)
Sulfuric acid, H <sub>2</sub> SO <sub>4</sub>	Infinity	Schwartz and White (1981) Durham et al. (1981)

## References

1. Laura Torrente-Murciano, Vince White, and David Chadwick. *Removal of SO<sub>x</sub> and NO<sub>x</sub> from Oxyfuel-Derived CO<sub>2</sub>*. in *IEA 1st Oxyfuel Combustion Conference*. 2009. Radisson Hotel, Cottbus, Germany.
2. White, V., et al., *Purification of Oxyfuel-Derived CO<sub>2</sub>*, in *9th International Greenhouse Gas Control Technologies*. 2008, Elsevier: Washington DC.
3. IPCC. *IPCC Fourth Assessment Report: Climate Change 2007 Synthesis Report*. 2007 [cited September 27, 2007]; Available from: [http://www.ipcc.ch/publications\\_and\\_data/publications\\_ipcc\\_fourth\\_assessment\\_report\\_synthesis\\_report.htm](http://www.ipcc.ch/publications_and_data/publications_ipcc_fourth_assessment_report_synthesis_report.htm).
4. IEA, *World Energy Outlook*. 2007, <http://www.worldenergyoutlook.org/2007.asp>.
5. Katzner, J., et al., *The Future of Coal- an interdisciplinary MIT study*. 2007.
6. *IEA Energy Technology Perspectives- Scenarios & Strategies to 2050*. 2010.
7. Wall, T., R. Stanger, and S. Santos, *Demonstrations of coal-fired oxy-fuel technology for carbon capture and storage and issues with commercial deployment*. *International Journal of Greenhouse Gas Control*, 2011. **In Press, Corrected Proof**.
8. CO2CRC. *Otway CO<sub>2</sub> Sequestration Project*. 2012 [cited; Available from: <http://www.co2crc.com.au/otway/>].
9. Wall, T.F., *Combustion processes for carbon capture*. *Proceedings of the Combustion Institute*, 2007. **31**(1): p. 31-47.
10. Jinying Yan, et al. *Flue Gas Cleaning Processes for CO<sub>2</sub> Capture from Oxyfuel Combustion - Experience of FGD and FGC at 30MWth Oxyfuel CO<sub>2</sub> Capture Pilot Plant*. in *IEA 1st Oxyfuel Combustion Conference*. 2009. Radisson Hotel, Cottbus, Germany.
11. Wuyin Wang and Jorgen Grubbstrom, *Flue Gas Cleaning in Oxyfuel Combustion*, in *IEA 1st Oxyfuel Combustion Conference*. 2009: Radisson Hotel, Cottbus, Germany.
12. McDonald, D.K. *Oxycombustion Considerations for FutureGen 2.0 Design*. Asia Pacific Partnership Oxyfuel Working Group Capacity Building Course 2011 [cited; Available from: <http://www.newcastle.edu.au/Resources/Projects/Asia%20Pacific%20Partnership%20Oxy-fuel%20Working%20Group/a%20Yeppoon%207%20McDonald%20Futuregen%202.0.pdf>].
13. Court, P., et al. *Callide CO<sub>2</sub> Capture Pilot Plant Design*. 2011 [cited; Available from: [http://www.ieaghg.org/docs/General\\_Docs/OCC2/Presentations/2\\_Callide%20CPU%20Design%20OCC2%2020110913.pdf](http://www.ieaghg.org/docs/General_Docs/OCC2/Presentations/2_Callide%20CPU%20Design%20OCC2%2020110913.pdf)].
14. Stanger, R. and T. Wall, *Sulphur impacts during pulverised coal combustion in oxy-fuel technology for carbon capture and storage*. *Progress in Energy and Combustion Science*, 2010. **37**(1): p. 69-88.
15. Cyril Thybault, et al. *Behaviour of NO<sub>x</sub> and SO<sub>x</sub> in CO<sub>2</sub> Compression/Purification Processes - Experience at 30MWth Oxy-coal Combustion CO<sub>2</sub> Capture Pilot Plant*. in *IEA 1st Oxyfuel Combustion Conference*. 2009. Radisson Hotel, Cottbus, Germany.

16. Kuhnemuth, D., et al., *Evaluation of Concepts for secondary SO<sub>x</sub> and NO<sub>x</sub> Removal from the Oxy-fuel Process*, in ICPWS XV. 2008: Berlin, September 8-11.
17. Thiemann, M., E. Scheibler, and K.W. Wiegand, *Nitric Acid, Nitrous Acid, and Nitrogen Oxides*, in *Ullmann's Encyclopedia of Industrial Chemistry*. 2000, Wiley-VCH Verlag GmbH & Co. KGaA.
18. Allam, R.J., E.J. Miller, and V. White, *Purification of carbon dioxide*. 2007, Air Products and Chemicals, Inc.: EP.
19. Counce, R.M. and J.J. Perona, *Scrubbing of gaseous nitrogen oxides in packed towers*. AIChE Journal, 1983. **29**(1): p. 26-32.
20. Sander, R., *Compilation of Henry's Law constants for inorganic and organic species of potential importance in environmental chemistry*. 1999, Max-Planck Institute of Chemistry: Mainz.
21. Pires, M. and M.J. Rossi, *The heterogeneous formation of N<sub>2</sub>O in the presence of acidic solutions: Experiments and modeling*. International Journal of Chemical Kinetics, 1997. **29**(12): p. 869-891.
22. Pettersson, T., et al. *Sulphur and Nitrogen Chemistry in Pressurized Flue Gas Systems*. in *2nd Oxyfuel Combustion Conference*. 2011. Yeppoon, Australia.
23. Nelo, S.K., K.M. Leskelä, and J.J.K. Sohlo, *Simultaneous oxidation of nitrogen oxides and sulfur dioxide with ozone and hydrogen peroxide*. Chemical Engineering & Technology, 1997. **20**(1): p. 40-42.
24. Daniel Koepke, et al. *Liquefaction of Oxyfuel flue Gas - Experimental Results and Comparison with Phase Equilibrium Calculations*. in *IEA 1st Oxyfuel Combustion Conference*. 2009. Redisson Hotel, Cottbus, Germany.
25. Tsukahara, H., T. Ishida, and M. Mayumi, *Gas-Phase Oxidation of Nitric Oxide: Chemical Kinetics and Rate Constant*. Nitric Oxide, 1999. **3**(3): p. 191-198.
26. Winkler, F., et al., *Cold DeNO<sub>x</sub> development for oxyfuel power plants*. International Journal of Greenhouse Gas Control. **5**, **Supplement 1**(0): p. S231-S237.
27. Joshi, J.B., V.V. Mahajani, and V.A. Juvekar, *INVITED REVIEW ABSORPTION OF NO<sub>x</sub> GASES*. Chemical Engineering Communications, 1985. **33**(1-4): p. 1-92.
28. Winkler, F., et al., *Cold DeNO<sub>x</sub> development for oxyfuel power plants*. International Journal of Greenhouse Gas Control, 2011. **In Press, Corrected Proof**.
29. Schwartz, S.E. and W.H. White, *Solubility equilibria of the nitrogen oxides and oxyacids in dilute aqueous solution*, in *Advances in Environmental Science and Engineering*, J.R. Pfafflin and E.N. Ziegler, Editors. 1981, Gordon and Breach Science Publishers: New York. p. 1 - 45.
30. Weisweiler, W., et al., *Absorption of NO<sub>2</sub>/N<sub>2</sub>O<sub>4</sub> in nitric acid*. Chemical Engineering & Technology, 1990. **13**(1): p. 97-101.